POLITECNICO DI TORINO

MASTER's Degree in Aerospace Engineering

MASTER's Degree Thesis

Effect of up and down reserve in off-grid power system planning

Supervisor

prof. GIOVANNI BRACCO

Co-Supervisor

ENRICO GIGLIO

Candidate

EDOARDO DESTRO

JULY 2024

Abstract

The growing integration of variable renewable energy sources (VRES) is steadily diminishing the capacity of conventional power plants to uphold grid stability. Consequently, alternative assets such as storage and control systems are essential to bridge the gap and uphold system stability. This study explores the impact of increasing vRES on Pantelleria island's off-grid power system. Through simulation and the integration of up and down reserves into the model, the research aims to comprehend the effects of down reserve requirements, starting from the formalization of the model variables and constraints. The model of the power system and the optimization problem is addressed using PYPSA, or "Python for Power System Analysis", an open-source software tool for the modeling and analysis of energy systems. This work aims to explore the impact of up and down reserves provided by Diesel generators, batteries, and energy conversion systems, as desalinators, in preserving stability within an off-grid environment amidst the increasing penetration of VRES.

Acknowledgements

Un doveroso grazie a tutt coloro che al Politecnico di Torino hanno reso possibile il mio percorso universitario. Ringrazio anche i miei relatori, senza i quali non sarebbe stato possibile lavorare a questa tesi.*

Grazie alla Fondazione ONAOSI e al Centro Formativo di Torino per tutto il sostegno e, soprattutto, per tutti i bellissimi ricordi.

Questo documento corona la fine di un lungo percorso la cui lunghezza non saprei come misurare. Alla mia famiglia. Ai miei amici. A tutti coloro a me cari. Grazie, a chi mi ha accompagnato.

Grazie, Elena, per il tuo calore e il tuo supporto.

Grazie anche a te, Mamma.

Table of Contents

List of Tables

List of Figures

Acronyms

VRES
: Variable Renewable Energy Source

FFG
: Fuel Fired Generator

BESS
: Battery Energy Storage System

IBR
: Inverter-Based Resources

SoC
: State of Charge

Li-ES
: Lithium-ion Energy Storage

PV
: Photovoltaic

FOWT
: Floating Offshore Wind Turbines

DGs
: Diesel Generators

WDeS
: Water Desalination System

NPC

Net Present Cost

RES

Renewable Energy Sources

VOM

Variable Operations and Maintenance

FOM

Fixed Operations and Maintenance

DSO

Distribution System Operator

RO

Reverse Osmosis

Nomenclature

$\dot{V}(t)$ flow of water at time t

η_s efficiency of the s-th BESS

Ω_G set of FFG

Ω_R Set of VRES

Ω_S Set of BESS

Ω_W Set of WDeS

A annualized capital costs

$c_{max,w}(t)$ maximum allowed filling percentage of the w-th WDeS

$C_{nom,w}$ nominal water volume capacity of the w-th WDeS

$c_w(t)$ volume of stored water of the w-th WDeS at time t

cc capital costs of the unit

CC_{tot} Total capital costs

$CF_r(t)$ capacity factor of r-th VRES source

chg index for the charging state of the BESS

$d(t)$ power output from the unit at time t

$d_s^{chg}(t)$ power flow in the s-th charge converter at time t

$d_s^{dis}(t)$ power flow in the s-th discharge converter at time t

dis index for the charging state of the BESS

$down$ subscript to indicate down reserve

dr discount rate

$e_s(t)$ available energy from s-th BESS at time t

$E_{c,w}$ energy consumption per cubic meter of desalinated water of the w-th WDeS

$e_{min,s}$ minimum SoC of the s-th BESS

E_{nom} nominal energy capacity

$EL(t)$ Power demand at time t

f_{obj} economic objective function

fix reserve requirement fixed quota related to generator failure

g subscript to indicate FFG units

ic specific idling cost of FFGs

oc operational costs of the unit

OC_{tot} Total operational costs

$p_{max}(t)$ maximum power output coefficient at time t

$p_{min}(t)$ minimum power output coefficient at time t

P_{nom} nominal power of the generator

$P_{r,av}(t)$ available power from r-th VRES source at time t

$q_g(t)$ down reserve by g-th FFG at time t

$q_s(t)$ down reserve by s-th BEES at time t

$q_w(t)$ down reserve by w-th WDeS at time t

$Q_{rq}(t)$ upper margin of the power down reserve at time t

r subscript to indicate VRES units

$r_g(t)$ up reserve by g-th FFG at time t

$r_r(t)$ up reserve by r-th VRES generator at time t

$r_s(t)$ up reserve by s-th BEES at time t

$r_w(t)$ up reserve by w-th WDeS at time t

$R_{rq}(t)$ upper margin of the power up reserve at time t

$s(t)$ binary variable for unit status (on or off)

s subscript to indicate BESS units

$sw(t)$ weight of the t-th time step

t time step taken into account

up subscript to indicate up reserve

$V_{\mathrm{nom},w}$ Water tank capacity in cubic meters

w subscript to indicate WDeS units

$w_{av,VRES}$ reserve requirement coefficient related to the VRES availability

w_{EL} reserve requirement coefficient related to the electrical load

Chapter 1

Introduction

The increasing penetration of variable renewable energy sources (VRES), is degrading grid stability due to their unpredictability. Nowadays, this represents one of the most significant barriers for VRES technologies such as photovoltaic and wind-turbines, limiting their integration into electric generation and undermining efforts in the energy sector transition [1]. The problem of VRES penetration concerns the decision-making process of grid operators regarding curtailing the amount of power injected into the grid from installations. As an example, a plant of any nominal power generally has a lower capacity factor, which refers to the portion of power available at a specific time and depends on the availability of the source. Because this fluctuates unpredictably over time, only a predetermined fraction of its capacity is normally accepted into the system - a process called dispatch.

With the increasing integration of renewable energy sources, managing reserves has become more challenging. Solar and wind power generation can be unpredictable, leading to periods of surplus or shortage that must be managed to prevent grid unbalances. Ensuring the balance between power generation and load demand is critical for maintaining the stability and reliability of the electrical grid. This balance is managed through a combination of "up" reserve and "down" reserve requirements.

Up Reserve Up reserves are the additional power supplies that can be quickly dispatched when there is an increase in demand or when a sudden drop in generation occurs. These reserves are crucial for addressing unexpected spikes in load or generation shortfalls. Usually, they need to be activated within minutes to seconds, depending on the grid's requirements. Technologies such as gas turbines, hydroelectric plants with fast ramp-up capabilities, and increasingly, battery storage systems, are commonly used [2].

Grid operators use forecasting tools to predict potential increases in demand, such as during extreme weather conditions or significant events that can cause load surges. Accurate forecasting helps in maintaining adequate up reserves [3]. In many regions, up reserves are procured through ancillary service markets. Power generators bid to provide reserve capacity, and operators select the most cost-effective options while ensuring reliability.

Down Reserve Down reserves involve the ability to reduce power output or absorb excess power from the grid when demand decreases or when there is an excess in generation, such as from variable renewable energy sources like wind or solar. It require flexible generation sources that can quickly reduce output without compromising operational integrity. This can include ramping down thermal power plants, curtailing renewable energy generation, or using demand response strategies where consumers reduce consumption. Energy storage systems, such as batteries and pumped hydro storage, play a crucial role in managing down reserves. They can absorb excess energy during low demand periods and release it when needed, thereby balancing the supply and demand [4].

The effective management of up and down reserves is essential for a resilient and reliable power system. Grid operators employ a range of strategies to balance these reserves and regulatory frameworks often mandate minimum reserve levels to ensure continuous reliability. By optimizing both up and down reserves, operators can ensure the seamless integration of renewable energy, minimize operational costs, and enhance the overall reliability of the power system.

Estimation of reserve requirements Considering reserve requirements at the energy planning stage is critical to the reliability of results. For example, inadequate modeling of these reserves can lead to underestimating the size of system components needed to balance supply and demand [5].
Historically, the two main sources of uncertainty were related to generator failures or load prediction errors. Reserve levels are therefore set with rules based on a fixed quota, related to the size of the largest generator, and a fraction of the total load. In contrast, the introduction of VRES into networks imposes more dynamic reserve requirements and must take into account their share [6]. Many proposed models can be found in the literature [7], but despite efforts, incorporating reserve requirements into planning models remains a complex task. For this reason, the formulation used in this study considers only the three main sources of uncertainty mentioned earlier, in order to save computational load so that the entire year can be simulated with hourly resolution.
Numerous studies, such as those cited later in the literature review, are currently

exploring ways to enhance renewable energy penetration, with energy storage systems, like batteries, emerging as a key solution. Other proposed measures include optimizing energy production across diverse sources, transitioning to fossil fuel generators with faster startup cycles, leveraging weather prediction algorithms, and implementing efficient power load management strategies [8]. Energy storage systems have been proposed to potentially mitigate instability-related issues by potentially decreasing reliance on conventional generators; however, batteries still represent an immature and therefore expensive solution, requiring careful planning. Moreover, due to the increasing complexity of the problem, the use of simulation software becomes essential, which further benefits from the contribution of such research to improve its effectiveness.

Minor islands, as off-grid systems, offer an ideal case study for energy planning research due to their isolated nature, limited land resources, abundance of renewable energy sources (RES), and pressing need for sustainable and reliable energy solutions. This study aims to analyze the combined impact of storage and VRES on the micro-grid electrical system of Pantelleria Island. Using PyPSA [9], an open-source tool for modeling and simulation of energy systems, data were generated in order to analyze how storage contributes to network stability by solving the system optimization problem. To accomplish this, both up and down reserve requirements have been incorporated into the optimization problem, formalizing all necessary equations and coding the constraints. The results encompass different scenarios, all based on an entire simulated year using the load curve of the Island.

Chapter 2

Literature Review

This chapter reviews several published research papers on VRES integration, focusing on three key areas of inquiry. The first section concern the integration of VRES, such as solar and wind power, and its implications for grid stability. The second segment evaluates the alternative assets, including energy storage systems and advanced control technologies, as potential solutions to mitigate grid stability. The third part provides an overview of the existing research landscape concerning the impact of VRES integration on off-grid power systems. For each of them, a brief summary of the results of various studies will be presented, focusing only on the aspects related to this study.

2.1 Integration of VRES and its impact on grid stability

As indicated by [1], the effects of wind uncertainty underscore the necessity of storage technologies to enhance wind turbine penetration. At the time of the research in 2019, significant improvements in terms of average annual mean capacity factors had not been achieved, and notable variability persisted in the US. Indeed, two parameters served as key indicators of wind plant performance: the average capacity factor over a year and the standard deviation of the capacity factor from high-frequency sampling. Both parameters influence the cost of electricity and enable the quantification of a specific plant's energy production. Additionally, they facilitate the attribution of energy storage costs to the individual plant.

The problems introduced by wind and solar installations - and some of the possible solutions - have been explored in [8]. This report describes the impacts caused by uncertainty in renewables, such as the ramp-up from the load coupled with a decrease in power availability from VRES. These kinds of events are difficult

to manage, especially in scenarios with high VRES penetration, and can particularly stress conventional fuel-fired generators (FFGs). In fact, older installations of FFGs usually need a longer time to shift power output and may even suffer from slow starting cycles.
Among the solutions presented in [8] there is the necessity of balance between photovoltaic and wind power production. The availability of these two sources can often alternate, thus improving reliability. The connection of renewable generators to the transmission grid rather than the distribution grid enhances real-time monitoring of electricity production data by operators . Investments in fossil fuel production technologies with faster start-up cycles, such as turbines and internal combustion engines, are also proposed. Additionally, the application of auxiliary technologies to renewable sources can mitigate electrical production variability. Increased demand flexibility, such as rapid cycles of appliance start-up and shutdown, is suggested to limit required power ramps.

The concept of flexibility in electrical systems, its sources, characteristics, and evaluation parameters, in relation to the increasing penetration of renewable energies is analyzed in [10]. They define four types of flexibility: power, energy, transmission, and voltage:

- Flexibility for power involves maintaining a balance between power supply and demand to ensure frequency stability during short-term intervals, typically ranging from seconds to hours.
- Flexibility for energy pertains to balancing the supply and demand of energy over medium to long-term periods, spanning from hours to several years. This necessity arises from a diminishing reliance on fuel storage-based energy generation.
- Flexibility for transfer capacity focuses on ensuring the smooth flow of power to prevent bottlenecks across short to medium-term periods, ranging from minutes to several hours.
- Flexibility for voltage concerns maintaining bus voltages within predefined limits over short-term duration, typically spanning from seconds to tens of minutes. This requirement stems from the rise of distributed generation within distribution systems, resulting in bi-directional power flow and varied operational scenarios.

The authors trace the historical development of flexibility, starting from its original definition and the current challenges posed by the uncertainty and variability of generation from renewable sources. They examine various sources of flexibility, such as conventional thermal generators, energy storage systems, demand management, and interconnections (including between different countries) of electrical systems. They also present the main parameters for measuring flexibility in conventional systems, such as reserve margin, start-up time, ramp rate, and marginal cost. Finally, they propose a classification of electrical systems based on their level of flexibility for the penetration of renewable energies.

2.2 Role of storage and control systems in mitigating grid stability issues

As already mentioned in the first section of this chapter, storage is considered one of the main solutions to the problem of grid stability. In this study, the primary reference will be to battery energy storage systems (BESS) when discussing storage. For thoroughness, it must be mentioned that "storage" refers to a type of technology that can be divided into several categories. [11] discusses the advancements and cost comparisons of various energy storage technologies. The review covers a range of technologies including stationary battery energy storage (such as Lithium-Ion and Redox Flow batteries), mechanical energy storage (such as Compressed Air Energy Storage and Pumped Storage Hydropower), and thermal energy storage (such as Super Critical CO2 Energy Storage and Molten Salt). It also discusses the services provided by energy storage systems, their direct and indirect benefits, and opportunities for integration with fossil thermal sources.

To effectively integrate batteries and maximize their benefits, they need to be connected in a way that allows for seamless interaction with the grid infrastructure. This typically involves two primary methods of connection: centralized and distributed as reported in [12]. In a centralized connection configuration, batteries are grouped together at a specific location within the grid, often at substations or power plants and this is the type of configuration considered in our grid model. These battery installations are typically large-scale and designed to provide significant energy storage capacity to support the overall grid operation. The connection to the grid is usually established through power converters or inverter-based resources (IBR) that convert the DC power output of the batteries into AC power compatible with the grid. Since all batteries are located in close proximity to each other, control and monitoring systems can be centralized, making it easier to manage the overall energy storage system. Large-scale installations can benefit from economies of scale, resulting in potentially lower costs per unit of energy storage capacity. Anyway, concentrating batteries in one location may lead to grid congestion issues, especially if the transmission infrastructure is not adequately sized to accommodate the increased power flow. They may be also vulnerable to single points of failure, which can disrupt grid operations if not properly mitigated.

In a distributed connection configuration, batteries are scattered throughout the grid at various locations, including residential, commercial, and industrial sites. These distributed energy storage systems are often smaller in scale but collectively contribute to enhancing grid stability and reliability. Each battery system is connected to the local distribution network and may be integrated with renewable energy sources or behind-the-meter applications. Distributed batteries provide localized support, reducing the risk of widespread outages due to localized disruptions. They offer flexibility in deployment, allowing utilities to target specific areas of the grid with high demand or stability issues. Additionally, batteries located at consumer premises can participate in demand response programs, helping to manage peak demand and reduce strain on the grid during periods of high usage. Some of the disadvantages concern the complexity of coordinating a large number of distributed battery systems, requiring sophisticated control and communication systems. Integrating numerous distributed systems into the grid may also pose challenges related to interconnection standards, grid compatibility, and safety regulations.

The article [13] provides an overview of the challenges and opportunities associated with the integration of IBR into electrical systems. It introduces the three existing typologies of IBRs (inverter grid-following, grid-supporting, and grid-forming) and discusses the issue of inertial response and frequency regulation. The text also analyzes transmission system stability, focusing on rotor angle control, frequency, and voltage regulation, using current real-world cases. Furthermore, it describes the difficulties in generating reliable models to manage critical events and coordinating between protection devices. The article proposes some possible solutions to address these challenges, including the use of advanced control and optimization algorithms, development of smart grids, adoption of harmonized technical standards, and updating of electrical system models and simulations.

2.3 Impact of VRES integration on off-grid power systems

An off-grid power system is a standalone electricity generation and distribution system that operates independently from the main electrical grid [14]. Unlike grid-connected systems, which rely on centralized power plants and transmission lines to deliver electricity, off-grid systems are designed to meet the energy needs of a specific location or community without any connection to external power sources. Off-grid power systems are mainly based on fuel-fired generators and, recently, also on renewable energy sources and energy storage solutions. Generators such as diesel generators are used year-round to provide most of the electricity output. Renewable energy sources such as solar panels, wind turbines, or micro-hydroelectric systems may be integrated to generate electricity locally. In addition to these primary generators and storage solutions, renewable energy sources can supplement the power supply, reducing reliance on fuel-fired generators and providing electricity during periods of sufficient renewable generation. The hope is that fuel-fired generators, as reliable source of power, will serve as backup generators when renewable resources are unavailable or insufficient to meet demand. Off-grid power systems could represent a perfect case study for the purpose of this research, in some cases they have already achieved 100% instantaneous penetrations from IBR based sources, as indicated by [13]. It is important to note that the controls and operations of microgrids are fundamentally distinct from those utilized by larger systems that include transmission networks.

The research [15] introduces a Modified Optimal Dispatch Strategy (MODS) aimed at solving the microgrid operational planning problem optimally. This approach combines the Load Following Dispatch Strategy (LFDS) and Cycle Charging Dispatch Strategy (CCDS) into a cohesive model. The problem is represented as a Mixed-Integer Linear Programming (MILP) model, incorporating MODS, LFDS, and CCDS, while also accounting for constraints related to DGs, BESS, and reserve requirements.
In contrast to simulation-based methodologies, this study employs a mathematical optimization technique, executed within the General Algebraic Modelling System (GAMS). The model is specifically designed for the day-ahead operational planning of a microgrid in South Sudan. MODS has been demonstrated to offer the most cost-effective daily operational plan when compared to LFDS and CCDS. The developed model has broad applicability for the day-ahead operational planning of various hybrid PV-Wind-Diesel-Storage microgrids, enabling operators to maintain system reliability through established reserve requirements.
A notable drawback of this research is the assumption of perfect accuracy in forecasted weather data and demand profiles, which does not account for the inherent uncertainties in renewable energy generation and demand fluctuations.

The research conducted by [16] proposes a comprehensive approach for planning and dispatching microgrids, with a focus on accurate cost modeling for fuel-fired generators and power reserve needs. It offers practical guidelines for designing and developing off-grid systems efficiently. Sensitivity analysis was conducted to evaluate various scenarios' impacts on system operation. Key findings include the importance of accurately modeling fuel-fired generator operations, considering power reserve requirements in system planning to prevent underestimation of demand and costs, and the significant cost savings and efficiency improvements achieved by incorporating storage technology for reserve supply. Storage not only

reduces overall system costs but also optimizes fuel-fired generator performance and reduces emissions. The research highlights the crucial importance of storage technologies in achieving a rapid, cost-effective, and efficient energy transition for off-grid systems.
This work employs similar assumptions and methodology to that of [16], welcoming its conclusion and exploring different reserve types, such as down reserve provided by BESS and desalinators.

Chapter 3

Methodology

3.1 Problem statement and research approach

This chapter explain the method used for model our case study of power grid while managing reserve demands and dispatch of the power sources. As described in the concluding part of the introduction, the aim is to investigate the impact of storage and VRES on micro-grid electrical systems utilizing PyPSA to generate the required data. The approach centers on devising systems with VRES, FFGs, and diverse storage options like BESS and Water Desalination Systems (WDeS). Specifically, for the considered system, different aspects of the model are investigated, as detailed below:

- propose the mathematical formulation of power reserve requirements and provision of power reserve by FFGs and storage for both up and down cases;
- present various scenarios, incorporating the following features:
  a) reserve requirements satisfied by FFGs alone;
  b) reserve satisfied by FFGs and storage together;
  c) the role of different storage alternatives in providing down reserve;

Each aspect outlined before has been incorporated incrementally, as illustrated in 3.1, to examine various combinations and investigate how those factors can influence energy planning for independent systems.

Costs, fuel consumption, and reserve availability were selected as some of the simplest and main factors to help evaluate the effects induced by the different scenarios. A couple of more factors, such as the computational weight and the system benefits has been analyzed. The former is deduced by measuring the time needed to complete the simulation, which is heavily affected by the tolerance

Case study		Up reserve			Down reserve			Code name scenario
		FFGs	BESS	WDeS	FFG	BESS	WDeS	
Base Scenario	*BS*							BS
Up Reserve Scenario	*Up FFG - RS*	x						UF_RS
	Up FFG Bess - RS	x	x					UFB_RS
	Up FFG Bess WDeS - RS	x	x	x				UFBW_RS
Up and Down Reserve Scenario	*Up&Down FFG - RS*	x			x			UDF_RS
	Up&Down FFG Bess - RS	x	x		x	x		UDFB_RS
	Up&Down FFG Bess WDeS - RS	x	x	x	x	x	x	UDFBW_RS
	Up FFG Bess, Down FFG WDeS - RS	x	x	x	x		x	UFBW_DFW_RS

Table 3.1: List of scenarios

chosen for the solver (the CPLEX solver V20.1.1 [17] and Gurobi V11.0 [18], two commercial softwares necessary to solve the optimization problems, were used). Instead, the benefits on the system are qualitative aspects that were traduced into problem statements:

1. cost-effectiveness of BESS vs WDeS;
2. stress on FFGs in term of work regimes;
3. stress on batteries in term of input/output power.

3.2 Mathematical formulation

This section describe the model variables and constraints that has been used to address the power reserve requirements, with emphasis on the formalization process.

3.2.1 Variables and conditions for up reserve

Formalization of the up reserve requirement To model the reserve requirement [16], the electrical load and the availability of VRES are taken into account through two coefficients $w_{EL,up}$ and $w_{av,VRES,up}$, which weigh their respective contributions for the up case. Additionally, a fixed quota fix_{up} is considered to account for uncertainty due to potential system failures. $R_{rq}(t)$ represents the upper margin of the power reserve to be made available in the case of ramp-up, therefore, its lower limit is defined as:

$$R_{rq}(t) = w_{EL,up} \cdot EL(t) + \sum_{r}^{\Omega_R} w_{av,VRES,up} \cdot P_{r,av}(t) + fix_{up} \tag{3.1}$$

Where $P_{r,av}(t)$ is calculated as:

$$P_{r,av}(t) = CF_r(t) \cdot P_{nom,r}, \quad \forall r \in \Omega_R \tag{3.2}$$

FFG up reserve supply At time t, the power reserve from the FFGs is determined by subtracting the power supplied to meet electrical demand from the maximum output of the i-th generator when activated:

$$r_g(t) \leq P_{nom,g} \cdot p_{max,g}(t) \cdot s_g(t) - d_g(t), \quad \forall g \in \Omega_G \tag{3.3}$$

BESS up reserve supply The limitation on the available power reserve $r_s(t)$ of a BESS at the $t-th$ time step arises from two primary factors:

$$r_s(t) \leq min\{r_{s,store}(t), r_{s,link}(t)\} \quad \forall s \in \Omega_S \tag{3.4}$$

The initial factor is determined by the BESS state of charge, which is subject to two constraints within the optimization framework. In the inequalities presented, $r_{s,store}(t)$ represents the discharge power available from storage unit s at time t, which can be provided over a duration of Δt.
Additionally, η_{dis} is the discharging efficiency of the BESS, $e_s(t)$ denotes the state of charge (SoC) of the BESS at time t, while $E_{nom,s}$ and $e_{min,s}(t)$ correspond to the nominal capacity and the minimum state of charge percentage, respectively. The influence attributed to the battery capacity can be described as:

$$r_{s,store}(t) \leq \eta_{dis,s} \cdot \frac{e_s(t) - E_{nom,s} \cdot e_{min,s}(t)}{\Delta t} \quad \forall s \in \Omega_S \tag{3.5}$$

$$\Delta t = (t+1) - t \tag{3.6}$$

The second restriction takes into consideration the rated power of the power electronics converter, as expressed by:

$$r_{s,link}(t) \leq P_{nom,s} \cdot p_{max,s}(t) - d_s^{dis}(t) \quad \forall s \in \Omega_S \tag{3.7}$$

Where $d_s^{dis}(t)$ indicates the power flow in the discharging link of the s-th battery at time t.

A third restriction is needed to ensure that the current outputs from all batteries do not exceed the C-rate limits of lithium batteries. The limits are derived from [19] to maintain consistency with the annualized capital and operational costs of BESS, which are also taken from the same paper. These costs apply to batteries with maximum continuous power outputs ranging between 6 hours and 1 hours (equivalent to 0.17C and 1C, respectively).

$$0.17 \leq \frac{P_{nom,s}}{E_{nom,s}} \leq 1 \quad \forall s \in \Omega_S \tag{3.8}$$

VRES up reserve supply At any given moment, the reserve that VRES can provide are limited by the maximum power available from the r-th generators. This restriction is determined by subtracting the power already utilized by each VRES technology from its available resource at that specific time:

$$r_r(t) \leq CF_r(t) \cdot P_{nom,r}(t) - d_r(t) \quad \forall r \in \Omega_R \tag{3.9}$$

Where $CF_r(t)$ is the capacity factor of the r-th generator, which is a coefficient between 0 and 1 representing the VRES availability of power at time t. Although, as highlighted in [16], the ability of VRES to provide up reserve has not been shown to be very effective. Therefore, the contribution from those sources to up reserves is neglected.

WDeS up reserve supply Lowering the desalination regime of the w-th WDeS allows for a reduction in the required power, which can be a contribution to the up reserve.

$$r_w \leq d_w(t) - P_{nom,w} \cdot p_{min,w}(t) \cdot s_w(t) \quad \forall w \in \Omega_W \tag{3.10}$$

Where $d_w(t)$ represents the electrical input of the w-th WDeS at time t, $P_{nom,w} \cdot p_{min,w}$ is the minimum power at which the desalination plant can operate, and $s_w(t)$ represents the status of the WDeS (on or off).

Condition for meeting up reserve requirements By taking into account all appropriate terms, the condition for meeting the lower limit of the up reserve is:

$$\sum_{g}^{\Omega_G} r_g(t) + \sum_{s}^{\Omega_S} r_s(t) + \sum_{w}^{\Omega_W} r_w(t) \geq R_{rq}(t) \tag{3.11}$$

3.2.2 Variables and conditions for down reserve

Formalization of the down reserve requirement The reserve requirement is symmetrically defined for both up and down cases with $Q_{rq}(t)$ representing the power reserve (to be absorbed) in the case of ramp-down. Again, the electrical load and VRES availability are taken into account through $w_{EL,down}$, $w_{av,VRES,down}$, and the fix_{down} quota. Thus, the lower limit of $Q_{rq}(t)$ is defined, similarly to $R_{rq}(t)$, as:

$$Q_{rq}(t) = w_{EL,down} \cdot EL(t) + \sum_{r}^{\Omega_R} w_{av,VRES,down} \cdot P_{r,av}(t) + fix_{down} \tag{3.12}$$

Where $P_{r,av}(t)$ is calculated as before.

FFG down reserve supply Lowering the throttle of the g-th generator allows it to absorb power (with the disadvantage of dissipating the energy instead of storing it). However, this still represents a contribution to the down reserve.

$$q_g \leq d_g(t) - P_{nom,g} \cdot p_{min,g}(t) \cdot s_g(t) \quad \forall g \in \Omega_G \tag{3.13}$$

Where $d_g(t)$ represents the output of the g-th generator at time t, $P_{nom,g} \cdot p_{min,g}$ is the minimum output at which the generator can operate, and $s_g(t)$ represents the status of the generator (on or off).

BESS down reserve supply Similarly to the up reserve, the capacity to provide reserve from the batteries is the minimum between the battery and the converter:

$$q_s(t) \leq min\{q_{s,store}(t), q_{s,link}(t)\} \quad \forall s \in \Omega_S \tag{3.14}$$

Defining the contribution due to the battery capacity as the power that can be absorbed in Δt amount of time, with $\eta_{chg,s}$ representing the charging efficiency of the BESS:

$$q_{s,store}(t) \leq \frac{1}{\eta_{chg,s}} \cdot \frac{E_{nom,s} \cdot e_{max,s}(t) - e_s(t)}{\Delta t} \quad \forall s \in \Omega_S \tag{3.15}$$

$$\Delta t = (t+1) - t \tag{3.16}$$

With the limitation due to the power converter as:

$$q_{s,link}(t) \leq P_{nom,s} \cdot p_{max,s}(t) - d_s^{chg}(t) \quad \forall s \in \Omega_S \tag{3.17}$$

Where $d_s^{chg}(t)$ indicates the power flow in the charging link of the s-th battery at time t.

VRES down reserve supply Variable renewable energy sources, such as solar and wind power, can pose challenges in terms of providing down reserves in energy power systems. The contribution from variable renewable energy sources to down reserves is not considered in this study.

WDeS down reserve supply Water production is extremely energy-intensive and can represent a source of reserve if properly managed. Every unit of water volume requires a certain amount of energy to be produced and stored. Because of this, the water tank can be seen as an energy storage unit. This energy can theoretically be converted back to electrical power, using the same principle as dams. However, our case study only considers the conversion from energy to water and not vice versa. That said, the capacity to provide reserve from water desalination is:

$$q_w(t) \leq E_{c,w} \cdot \frac{C_{nom,w} \cdot c_{max,w}(t) - c_w(t)}{\Delta t} \quad \forall w \in \Omega_W \tag{3.18}$$

Where $E_{c,w}$ is the energy consumption per cubic meter of desalinated water, measured in kWh/m^3, $C_{nom,w}$ is the nominal water volume capacity, $c_{max,w}(t)$ is the maximum allowed filling percentage, and $c_w(t)$ is the actual volume of water stored at time t.

The second restriction takes into consideration the rated power of the installed WDeS, as expressed by:

$$q_w(t) \leq P_{nom,w} \cdot s_w(t) - d_w(t) \quad \forall w \in \Omega_W \tag{3.19}$$

Where $P_{nom,w}$ is the rated power production capacity, $d_w(t)$ indicates the power flow of the w-th desalinator at time t, and $s_w(t)$ represents the status of the desalinator (on or off).

Condition for meeting down reserve requirements Similarly to the up reserve, the condition for meeting the lower limit of the down reserve is as follows:

$$\sum_{g}^{\Omega_G} q_g(t) + \sum_{s}^{\Omega_S} q_s(t) + \sum_{w}^{\Omega_W} q_w(t) \geq Q_{rq}(t) \tag{3.20}$$

3.3 PyPSA for modeling and analysis of energy systems

PyPSA [9], short for "Python for Power System Analysis," is an open-source Python package designed for the modeling and analysis of energy systems, with a primary focus on electricity networks. It provides a comprehensive framework for simulating and optimizing various aspects of power systems, including generation, transmission, distribution, and consumption.

PyPSA offers a high degree of flexibility, allowing users to model diverse energy system configurations, from small-scale microgrids to large interconnected grids. Its modular design enables users to customize models according to specific requirements and integrate various renewable and conventional energy sources. It also incorporates a wide range of functionalities essential for energy system analysis, including optimization algorithms, economic dispatch models, network flow analysis, and capacity expansion planning. In fact, is designed to work alongside other popular Python libraries and optimization solvers, facilitating integration with existing modeling frameworks and data analysis workflows.

Being open-source, it encourages collaboration and transparency within the energy modeling community. Users can access the source code, contribute improvements, and adapt the software to address evolving research needs and industry challenges. Its open-source nature and integration capabilities make it well-suited for addressing diverse research questions, informing policy decisions, and supporting the transition towards sustainable and resilient energy systems.

3.4 Addressing the optimization problem with PyPSA

As previously mentioned, PyPSA can optimize the operation of generation assets and energy storage systems on energy networks. To achieve this, the first necessary step is to model the existing power system on Pantelleria Island. This process is explained in the appropriate chapter and involves gathering data on the power generation assets, energy storage systems, and the demand profile of the Island.

Once the model network is available, every time the power system optimization function is called, the software automatically sets up the problem to achieve the objective. The details of how the optimization problem is constructed and solved are omitted because they are beyond the scope of this document. However, power system optimization allow us to determine the optimal dispatch of generation assets that minimizes capital and marginal costs. Some examples include the minimum sizes of components which are declared as "extendable", the power flow between the network lines, or when to charge/discharge batteries.

The economic objective function adopted consists of the Net Present Cost (NPC) of the power system. A description of how this is formalized, within the context of PyPSA, is available in the documentation at the link *pypsa.readthedocs.io*. In our case, it considers the total annualized capital costs CC_{tot} and total operational costs CO_{tot} of VRES techs, BESS, and FFGs as reported in the Equations 3.21 to 3.23.

$$\min f_{\text{obj}}^{\text{base}} = \min\{CC_{\text{tot}} + OC_{\text{tot}}\} \tag{3.21}$$

$$
\begin{aligned}
CC_{\text{tot}} = & \sum_{g}^{\Omega_G} cc_g \cdot P_{\text{nom},g} + \sum_{r}^{\Omega_R} cc_r \cdot P_{\text{nom},r} + \\
& \sum_{s}^{\Omega_S} cc_s \cdot E_{\text{nom},s} + cc_{s,\text{links}} \cdot P_{\text{nom},s} + \\
& \sum_{w}^{\Omega_W} cc_w \cdot V_{\text{nom},w}
\end{aligned} \tag{3.22}
$$

$$
OC_{\text{tot}} = \sum_{t}^{t_{\text{end}}} sw(t) \cdot \left(\sum_{g}^{\Omega_G} oc_g \cdot d_g(t) + s_g(t) \cdot ic \cdot P_{\text{nom},g} + \sum_{s}^{\Omega_S} oc_s \cdot d_s(t) \right) \tag{3.23}
$$

Where cc stays for capital costs, oc for marginal costs, $sw(t)$ is the weight of the t-th time step, s_g is the status of the g-th FFGs, ic is the specific idling cost, and $V_{\text{nom},w}$ is the water tank capacity in m^3. The NPC is a financial metric used to evaluate the cost of a power system or energy project over its entire lifetime. It represents the present value of the costs considering the discount rate. A lower NPC is typically desirable and indicates lower costs. It's a way to compare different investment options by considering all costs and benefits over time.

The discount rate is an essential parameter for investors and policymakers to ensure accurate project valuation and decision-making. For renewable energy systems (RES), it can vary depending on several factors [20], including the country or region where the technology is being implemented, the specific type of RES technology, and the prevailing economic conditions.

By default, the power system optimization does not consider any reserve requirements but only represents the best solution given the conditions. For this reason, it was needed to incorporate the reserve requirements that were formalized beforehand through their equations. The details of this process are discussed in the chapter 4.

Chapter 4

Model Development

4.1 Description of the power system model of Pantelleria

The island of Pantelleria, situated in the Strait of Sicily, is a remote, unconnected small island spanning 85 km^2. With a stable population of 7700 inhabitants and significant tourist influxes during the summer months, it serves as an exemplary case for investigating local energy autonomy through the utilization of a microgrid energy planning model [21].

4.1.1 Cost assumptions

As described in the previous section, to apply the NPC equations, the model must also consider economic differences between DGs, RES technologies, and WDeS. Because DGs and RES are directly related to energy production, whereas WDeS relates to water production, their economic parameters are discussed separately.

FFG and VRES costs Both FFG and VRES have initial capital costs, but only FFG presents marginal costs related to the amount of power they deliver, as they are directly proportional to the fuel consumed. On the other hand, RES operational costs are only related to maintenance since they do not consume any fuel. In our simulations, DG generators are pre-installed and cannot be expanded, meaning only their operational costs are considered. The capital and operational expenses for the selected RES technologies are detailed in the table 4.1.

Technology	Capital C.	Operational C.	Op. Lifetime
PV	905 $\frac{€}{kW}$	17 $\frac{€}{kW \cdot y}$	25 years
FOWT	4.500 $\frac{€}{kW}$	94 $\frac{€}{kW \cdot y}$	25 years
Li-ES	300 $\frac{€}{kWh}$	35 $\frac{€}{kWh \cdot y}$	15 years
Power Converter	150 $\frac{€}{kW}$	18 $\frac{€}{kW \cdot y}$	15 years

Table 4.1: Cost assumptions related to RES technologies. References in Section 4.1.2

WDeS costs The only WDeS-related costs that have been considered in this study are the capital costs of water reservoirs; the estimate can vary greatly because it depends largely on the location and size of the reservoir and related project. The value was selected from [22], the source is based on a survey of ground-level concrete storage tanks used in South Australia.

Water tank capital c.	Op. Lifetime
500 $\frac{€}{m^3}$	20 years

Table 4.2: Cost assumptions related to WDeS. References in Section 4.1.2

Once defined, all capital costs are calculated using the fixed-rate mortgage formula, assuming a discount rate of 5% [23], and their operating lifetime.

$$A = cc \cdot \frac{dr(1 + dr)^n}{(1 + dr)^n - 1} \tag{4.1}$$

Where cc represents the capital cost, dr represents the discount rate and n the number of years. When considering the operational costs of RES, variable operations and maintenance (VOM) and fixed operations and maintenance (FOM) costs are typically expressed in $\frac{€}{kW \cdot y}$ and do not need to be annualized.

4.1.2 Network model

The model architecture depicted in Figure 4.1 includes a system composed of Lithium-ion Energy Storage (Li-ES), Photovoltaic (PV) arrays, Floating Offshore Wind Turbines (FOWT), diesel generators (DGs), and a water desalination system (WDeS). Detailed descriptions of each component are provided in the subsequent paragraphs.

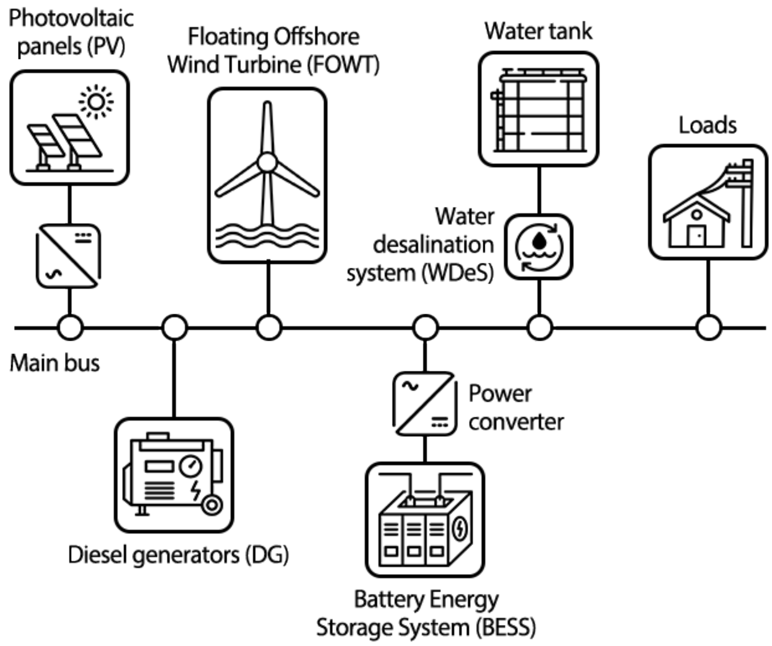

Figure 4.1: Model architecture. Images from Flaticon.com

Wind RES Parameters The maximum wind capacity was limited to 10MW and can only be constituted by offshore turbines; onshore plants are excluded due to local legal restrictions [24]. The local wind energy production data are collected through different sources such as renewables.ninja [25, 26] and the ERA5 web platform [27]. FOWT capital and operation costs where obtained from [28].

PV RES Parameters The maximum PV capacity was limited to 15MW. The local solar energy production data are collected through different sources such as renewables.ninja [25, 26] and the ERA5 web platform [27]. PV capital and operational costs were obtained from [29, 30]. Capital and operational costs include all the necessary equipment, such as power converters, for operating the energy storage system.

Li-Es Parameters The maximum BESS capacity was limited to 50MWh. Because batteries, particularly lithium-ion batteries, pose challenges in accurate modeling, certain aspects need to be simplified to conserve computational resources. A constant standing loss of 0.3% of energy loss per day [31] and a constant round-trip efficiency of 90% [32] was used. The state of charge (SoC) of the Li-ES system is assumed to be balanced, ensuring that the initial and final SoC levels are equal in every simulation. Costs were obtained from [19].

DGs Parameters The island's current energy system consists of eight diesel generators (DGs) with nominal capacities between 1.2 MW and 5.3 MW, resulting in a total installed capacity of 25 MW. Further details, including diesel costs and generator sizes, can be found in [16], based on data sheets from the local Distribution System Operator (DSO).

WDeS Parameters Two reverse osmosis (RO) desalinators plants are installed on Pantelleria, which consume approx. $E_c = 3.5\ kWh/m^3$. The Sataria plant has 4 watermakers of 1400 m^3/day, and the Maggiuluvedi plant has 1 watermaker of 1000 m^3/day. They feed, respectively, the Kaffefi, Gelsiffer and Scauri reservoirs, and the tankers located at Arenella. The existing total water storage capacity is about 24950 m^3 [33]. This volume is set as the initial value for each simulation, although the model is able to modify this capacity.
The desalinators were modeled as a single unit with a fixed capacity of $\dot{V}_{max} = 275\ m^3/h$, obtained by adding the daily production capacities of the Sataria and Maggiuluvedi plants and calculating the average to obtain a constant hourly production. This unit, corresponding to $P_{max} = 0.9625\ MW$ (equation 4.2), is connected to a single nearby water tank.

$$P_{max} = \dot{V}_{max} * E_C * 10^{-3} \tag{4.2}$$

Electrical Load Parameters The load profiles were once again provided by the local DSO. The annual electricity demand in 2019 was approximately 37 GWh [34], with a peak load of 9.5 MW and a base load of 2.2 MW. The equivalent electrical load for water production was subtracted from the Island load profile.

Water Load Parameters The water production curve, available at [21], was utilized to model water consumption, and the water demand was set to be constant throughout each day of each month.
Using the appropriate function of PYPSA, the water vector was added to the network, which differentiates the network components working with electricity from those working with water; Figure 4.2 illustrates the concept. Through the water bus, the following equation must be met:

$$\dot{V}_{load}(t) = \dot{V}_{WDeS}(t) + \dot{V}_{tank}(t) \tag{4.3}$$

Where $\dot{V}(t)$ denotes the flow of water in m^3/h. It is important to note that $\dot{V}_{tank}(t)$ can be positive (when emptying) or negative (when filling), and $\dot{V}_{WDeS}(t)$ can be only zero or positive. The water flow is decided according to the best condition for the system, respecting the imposed limits.

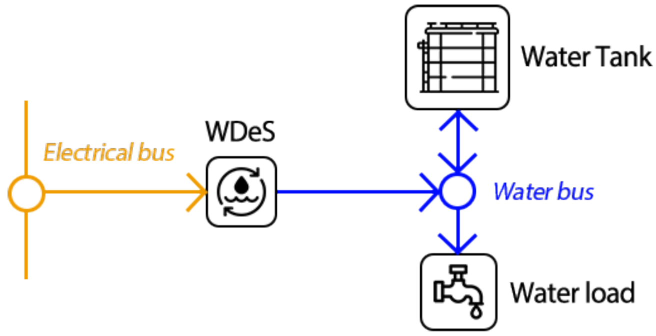

Figure 4.2: Model representation of WDeS, Tank and Water Load connected to the network. Images from Flaticon.com

4.2 Explanation of the integration of up and down reserves into the model

All the conditions presented in section 3.2 have been included into the optimization problem using the Linopy [35] module within PyPSA. For each of the conditions, a specific variable has to be declared and the relative constraint was implemented. The "extra" constraints were made declarable through specific functions in order to simplify the setup of each scenario.

For all simulated scenarios, the values chosen for the parameters w_{EL}, $w_{av,VRES}$, and fix, as presented in subsections 3.2.1 and 3.2.2, are displayed in Table 4.3.

Parameter	Up Res. Req.	Down Res. Req.
w_{EL}	10%	10%
$w_{av,VRES}$	10%	10%
fix	min(Pmax,g)	min(Pmax,g)

Table 4.3: Values of reserve requirement parameters

Processing the results of a simulated year, the code was tested with two methods:

- Method of reserve surplus: calculating the difference between the actual reserve from each component and the reserve requirement ($R_{rq}(t)$ and $Q_{rq}(t)$). If the requirement is met, the reserve must be positive or closer to zero than the imposed tolerance at every time step.
- Method of inequality check: verifying that each term ($r_g(t)$, $q_g(t)$, $r_s(t)$, and $q_s(t)$) respects its own inequality within the imposed tolerance.

4.3 Discussion and Limitations on the Representation of Assets

This study use a MILP model to balance computational complexity and result accuracy. This section illustrates the main limitations of the model that emerged during the course of the study.

VRES PV panels are modeled as if they were all located at a representative geographical point on the island with the highest efficiency tilt, disregarding differences arising from terrain or installations.
Conversely, the power outputs of FOWT depend on various factors, such as the wind turbine model, manufacturer, blade diameter, and rated capacity. It is assumed that the characteristics of the wind turbine remain constant, opting for a specific representative model with a 5MW power output.

BESS In [19], VOM are considered zero, consolidating all operational costs into FOM, assuming approximately one cycle per day. Both capital and operational costs are expressed for usable capacity, ensuring the BESS can provide nominal performance throughout its operational life. Consequently, the battery is assumed capable of delivering its entire nominal capacity, neglecting maximum and minimum safe discharge depths.
The round-trip efficiency of the BESS is heavily influenced by the power delivered, as highlighted by [36]. Battery stress is analyzed in terms of power delivered and absorbed, with results discussed in the appropriate section, but the round-trip efficiency is considered to be constant.

WDeS Only the water tank capacity was set to be extendable, with WDeS modeled as those already existing on the island. This decision was made solely to investigate the reserve provision of water storage, rather than the impact of plant expansion. The system was modeled as being able to operate from 0 to maximum installed power, neglecting a minimum power limit, assuming constant efficiency for any production regime and always active throughout the year.
It has been decided to simulate scenarios to compare only the reserve availability without penalizing the desalination plant with production-related costs. This choice was made for simplification reasons, as operational costs include a wide range of elements (as power, chemicals, labor, and replacement of membranes and filters) [37] which are related both to technological and purely economic reasons, such as the costs of consumed electricity. Therefore, in this study, the desalination plant is represented as a tool for managing stability integrated into the electrical system, interpreting the results as referring to the "best possible case" without accounting

for desalination costs.
When considering the energy consumption per cubic meter of WDeS, the power needed to pump water far away from the plant location is neglected. All water tank capacities are modeled as if they were located in proximity to the desalinator. Because the water production was originally included in the electrical load of the island, its power consumption is subtracted from the load supposing a constant water request through all day. The constant water "spillage" from the tanks is calculated as the average from the monthly water consumption. Sanitary requirements of water production, such as stagnation limits for drinking water, have been neglected. The capital costs of water tanks vary greatly depending on the dimensions of the installation. As the Island's storage capacity comprises multiple tanks, the price was chosen from the upper limit.

Chapter 5

Results and Analysis

5.1 Presentation and analysis of simulation results

The main results of all simulated scenario are presented in the tables 5.1, 5.2 and 5.3.

Scenario	MIP relative gap	Comp. time (sec)
BS	0.0159	203.13
UF_RS	0.0300	>60000
UFB_RS	0.0163	4716.61
UFBW_RS	0.0189	685.13
UDF_RS	0.0427	66177.43
UDFB_RS	0.0198	941.72
UDFBW_RS	0.0187	950.26
UFBW_DFW_RS	0.0195	25397.92

Table 5.1: Final tolerance and calculation time for each result

Scenario	f.obj(M€/y)	PV gen.(MW)	FOWT gen.(MW)	BESS(MWh)	BESS conv.(MW)	Tank size(m^3)
BS	8.89	15.0	3.8	27.5	6.9	24950.0
UF_RS	10.75	15.0	2.7	25.8	5.6	24950.0
UFB_RS	8.95	15.0	3.9	26.9	6.2	24950.0
UFBW_RS	8.95	15.0	4.0	28.1	7.1	24950.0
UDF_RS	15.81	8.1	1.3	11.0	2.5	24950.0
UDFB_RS	9.19	15.0	4.1	30.4	9.3	24950.0
UDFBW_RS	9.09	15.0	4.0	29.3	8.5	24950.0
UFBW_DFW_RS	13.2	11.6	1.9	24.6	5.4	24950.0

Table 5.2: Main sizes of network components

Scenario	VRES penet.	FOWT curt.	PV curt.	DGs work.h.	WDeS work.h.
BS	86%	17%	17%	3025.0	4404
UF_RS	79%	18%	14%	12702.0	4681
UFB_RS	86%	15%	20%	3019.0	4513
UFBW_RS	86%	26%	14%	3197.0	4435
UDF_RS	38%	15%	24%	17397.0	4828
UDFB_RS	86%	26%	15%	3260.0	4450
UDFBW_RS	86%	25%	15%	3201.0	4606
UFBW_DFW_RS	55%	12%	25%	9832.0	7510

Table 5.3: VRES penetration, PV and FOWT curtailment and cumulative working hours for DGs and WDeS (where WDeS working hours refer to non-zero power output from the desalinator)

Scenario	DGs tot.en.(MWh)	FOWT tot.en.(MWh)	PV tot.en.(MWh)
BS	6007	20419	11020
UF_RS	8400	21331	7775
UFB_RS	6045	19759	11619
UFBW_RS	5821	21218	10395
UDF_RS	23141	10134	3761
UDFB_RS	5759	21125	10547
UDFBW_RS	5877	21114	10445
UFBW_DFW_RS	17220	14323	5904

Table 5.4: Total energy supplied by DGs, FOWT and PV

As can be seen from table 5.1, looking at the time it took to solve UF_RS and UDF_RS (the scenarios in which reserve requirements were met only by FFGs), it is evident how demanding these two scenarios are in terms of computational resources. To overcome this problem, it was necessary to expand the MIPGAP tolerance by more than 2% in order to converge on a solution.

Our baseline reference is represented by BS (which stands for Basic Scenario), as it depicts results for a perfectly optimized system where the DSO could predict future load and VRES power availability accurately. In contrast, each other scenario introduces constraints to account for the inherent unpredictability of the system, leading to economically sub-optimal performances compared to BS. These cost differences are better illustrated in Figure 5.1.

It is also immediately apparent how deleterious it is to rely solely on DGs to meet the reserve (UDF_RS), as this would involve suppressing overvoltages by reducing or shutting down DG generators, which means that a sufficient number of them need to be always active in case of load fluctuations. Though, the VRES penetration value of 38% in UDF_RS, compared with 75% of UF_RS, is more

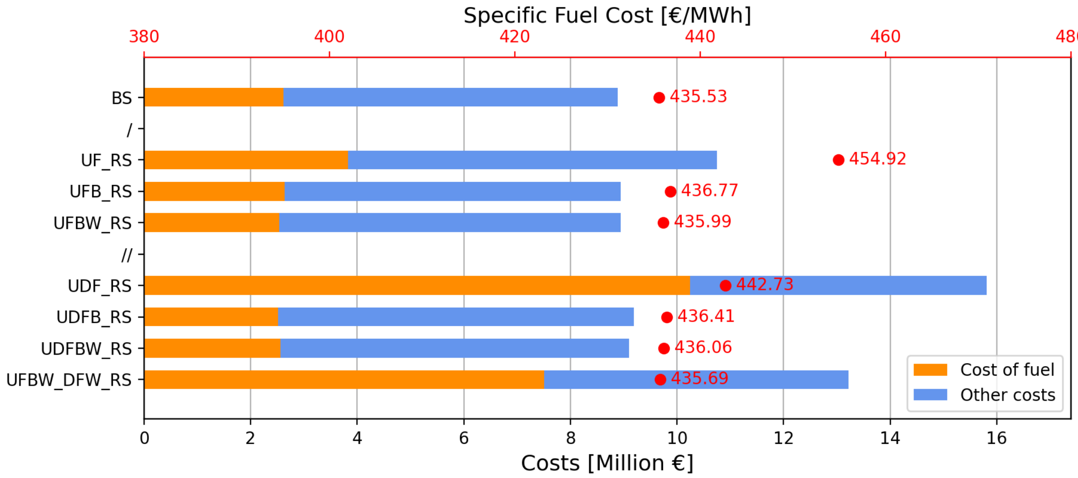

Figure 5.1: Objective function results and marginal costs of DGs (lower scale). Specif fuel consumption (upper scale)

reminiscent of real case penetration percentages that are reported in the literature [10]. Finally, UFBW_DFW_RS also does not seem to be an optimal choice in terms of absolute cost. However, as evidenced by the specific fuel cost, the DGs are operated more efficiently in this scenario, which is also confirmed in the next section.

5.2 Effects of reserve requirements on Pantelleria island's off-grid power system

One important aspect to notice is the difference in the size of network components between the "parallel" scenarios considering only up reserve and those considering both up and down reserve together. For instance, UFB_RS and UDFB_RS represent simulations where reserve requirements are constrained to be satisfied only by FFG and BESS: in UFB_RS the constraints are applied only for the up reserve, while UDFB_RS applies the constraints for both up and down reserve, as shown in Table 3.1.
Because the stability of the network cannot disregard either up or down reserve, simulating a scenario with only one of them may lead to an underestimation of certain aspects. This is illustrated in Figure 5.3, which shows the variations from the BS results (where a positive 50% means that the scenario's value has increased to 1.5 times the BS value) and helps visualize how simulations with only up reserve constraints tend to underestimate BESS in terms of both energy capacity and power.

The most obvious case is that of UFB_RS and UDFB_RS, where there are negligible or minor differences between PV and FOWT nominal power but significant differences in BESS energy and power capacity. From Table 5.3, it is noticeable that the VRES penetration remains identical, but in UFB_RS, the power from PVs was curtailed more than FOWT, whereas the reverse happened in UDFB_RS. The reversal in the trend for PV and FOWT curtailment is best illustrated in Figure 5.2. This change seems to be correlated with the reliance on DGs and battery energy capacity. The more the system relies on DGs, the less it relies on VRES, leading to an optimal economic result with a smaller battery size.

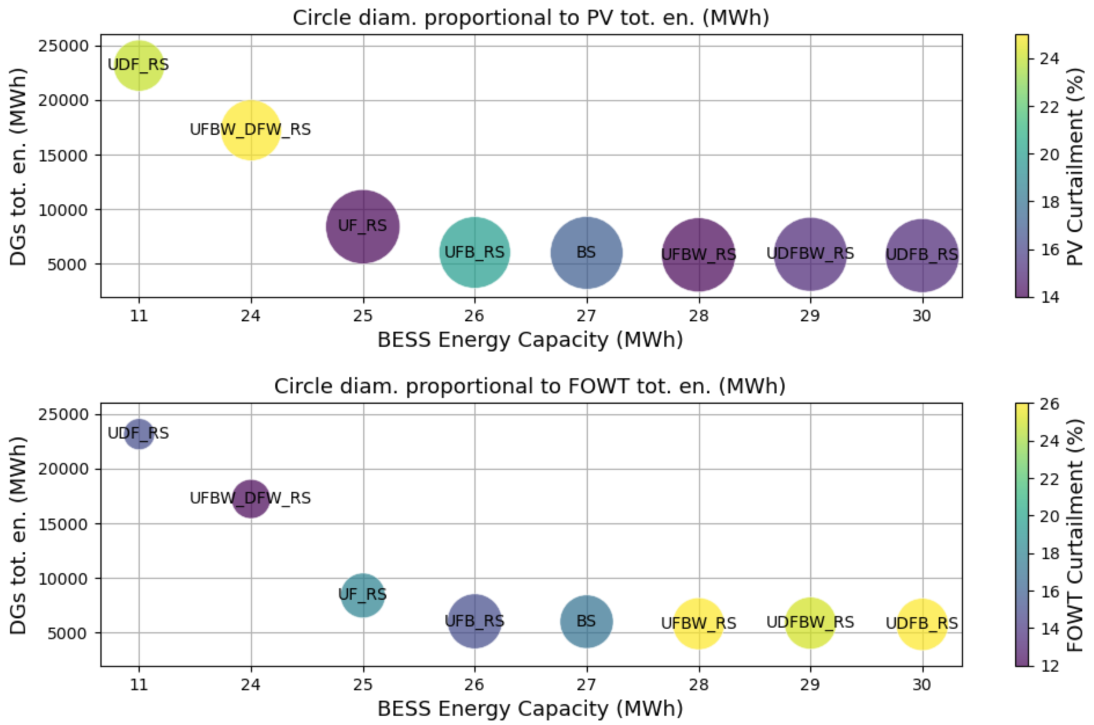

Figure 5.2: Scatter plot of PV vs FOWT curtailment. The x-axis represents BESS energy capacity, the y-axis shows the total energy supplied by DGs, the color map indicates the curtailment level, and the circle diameter is proportional to the total energy supplied.

As already mentioned, Table 5.3 shows how VRES penetration is drastically reduced for UDF_RS (where reserves is satisfied solely by DGs) and UFBW_DFW_RS (where BESS constraints are removed from the down reserve). In these scenarios, the costs in terms of fuel consumption are evident and are not offset by the reduction in installed VRES nominal power and BESS capacity, as shown in Figure 5.3. Scenarios UDFB_RS and UDFBW_RS show that the impact of BESS and WDeS leads to a partial restoration of the BS system's optimal conditions, with the role of WDeS in UDFBW_RS appearing to alleviate the power capacity requirements of BESS.

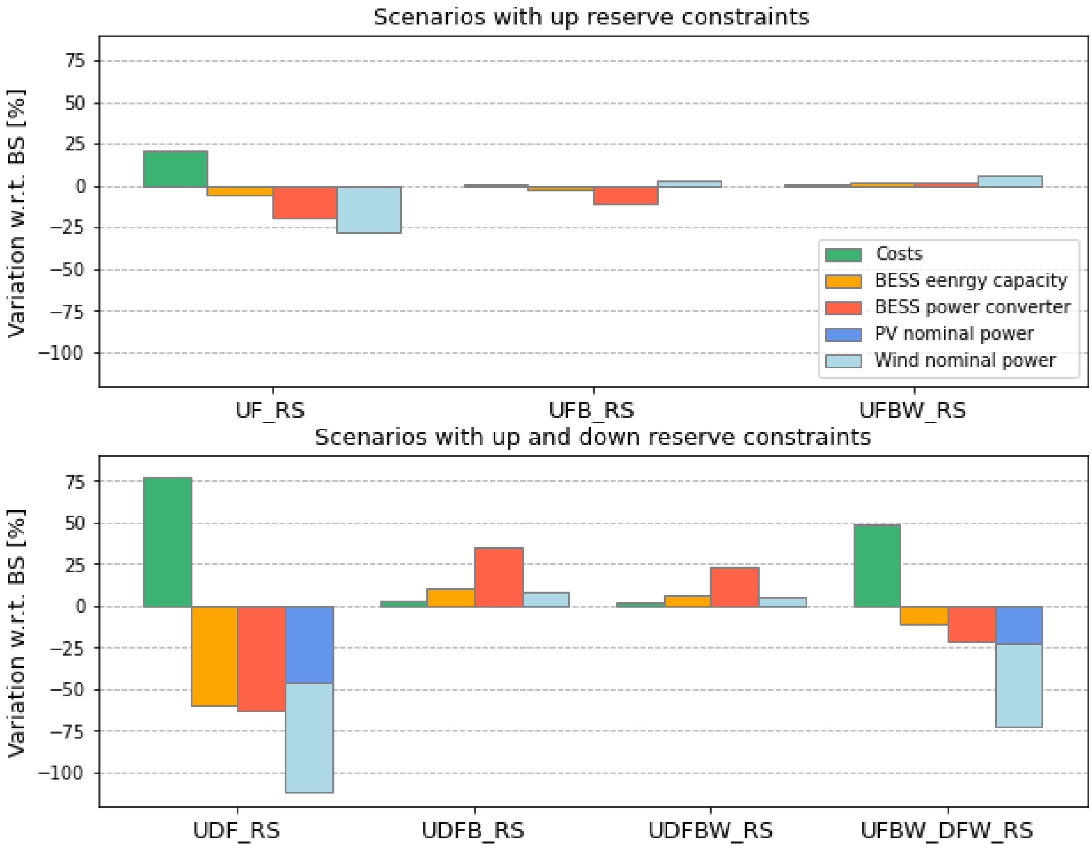

Figure 5.3: Results comparison between scenarios. All % variations refer to the BS scenario results.

Another aspect attempted to be estimated is the stress on batteries presented by each scenario. Figure 5.4 is used to estimate battery charge/discharge power stress. This shows no concerning values for any scenario except UDF_RS, where the limited battery size, compared to other scenarios, could explain the result. However, it is important to remember that in all simulations the power converters were limited to remain below the maximum safe discharge rate for the installed BESS (also referred as C rate), and that our model considers a constant round-trip efficiency regardless of power input/delivery.

Finally, the stress on DGs can be assessed by plotting the distribution of power delivered when they are active, as depicted in Figure 5.5. Again, the results show

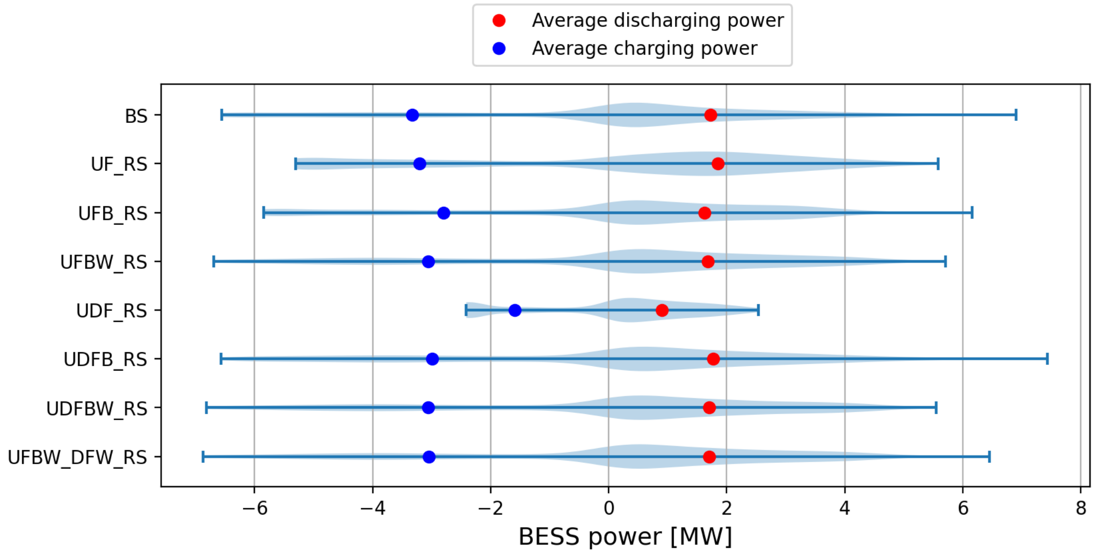

Figure 5.4: Violin plot and average power of the BESS system

that UDF_RS does not represents an efficient scenario, while UDFB_RS and UDFBW_RS are very similar and show strong improvements over UDF_RS. If BESS is excluded from the down reserve (UFBW_DFW_RS), the system still relies largely on DGs, but is now able to operate at much better regimes.

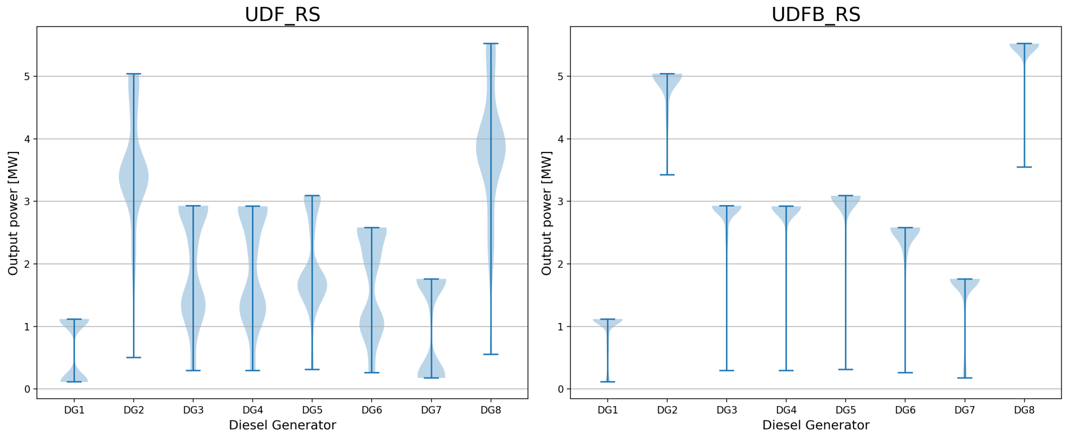

(a) **(b)**

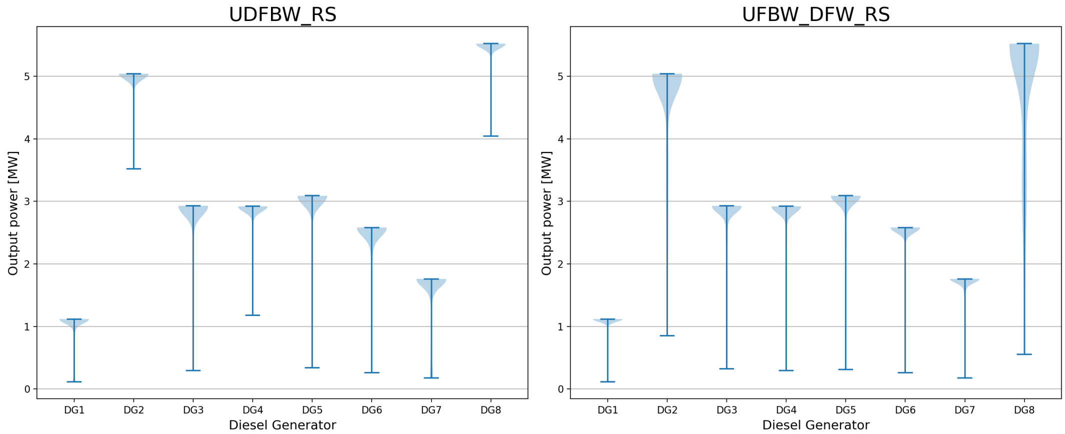

(c) **(d)**

Figure 5.5: Violin plot of DGs power output

5.3 Contributions of DGs, BESS, and WDeS to stability preservation

To analyze each technology's contribution to reserve provision, two different perspectives can be employed:

- Calculate the average reserve provided by each technology at each hour of the day, as illustrated in Figures 5.6.
- Plot the color map of the reserve provided at each time step, as illustrated in Figures 5.9.

The average reserve for each hour of the day throughout the year can help visualize how the system operates. This consistency is evident in 5.7, where it is possible to observe that the differences in reserve availability between seasons are mainly due to differences in magnitude rather than in their distribution during the hours of the day. Additionally, 5.9 helps visualize this pattern, illustrated by the central stripe of a different color representing in (a) the midday peak of up reserves and in (b) the bottom of down reserves. Thus, figure 5.6 helps illustrate the underlying "logic" repeated in each scenario, where the battery charging phase and water production aligns with daylight hours, maximizing PV utilization. Consequently, this leads to increased up reserve availability and reduced down reserve during midday hours. The only "outlier" scenario with regard to water production is UFBW_DFW_RS, where both DGs and WDeS are forced to operate more continuously throughout the entire 24 hours, also demonstrated by the hours of operation in the Table 5.3.

The UDF_RS scenario mandates DGs to operate with at least 100% reserve coverage (where reserve percentage is the ratio of available reserve to requirement R_{rq} or Q_{rq}). For this reason, the system reduces the BESS capacity to achieve savings, thereby impacting their potential to provide reserves (illustrated by lighter colors indicating available reserves that have not been constrained).
The limited reserve availability of UDF_RS is also highlighted in 5.8, which shows the reserve surplus for all hours of the year. The reserve surplus is the difference between total available reserve - in this case from DGs, BESS, and WDeS excluding VRES - and the related R_{rq} or Q_{rq} requirement.

As can be seen from all the figures, the technology with the greatest reserve availability in both up and down obviously remains BESS.

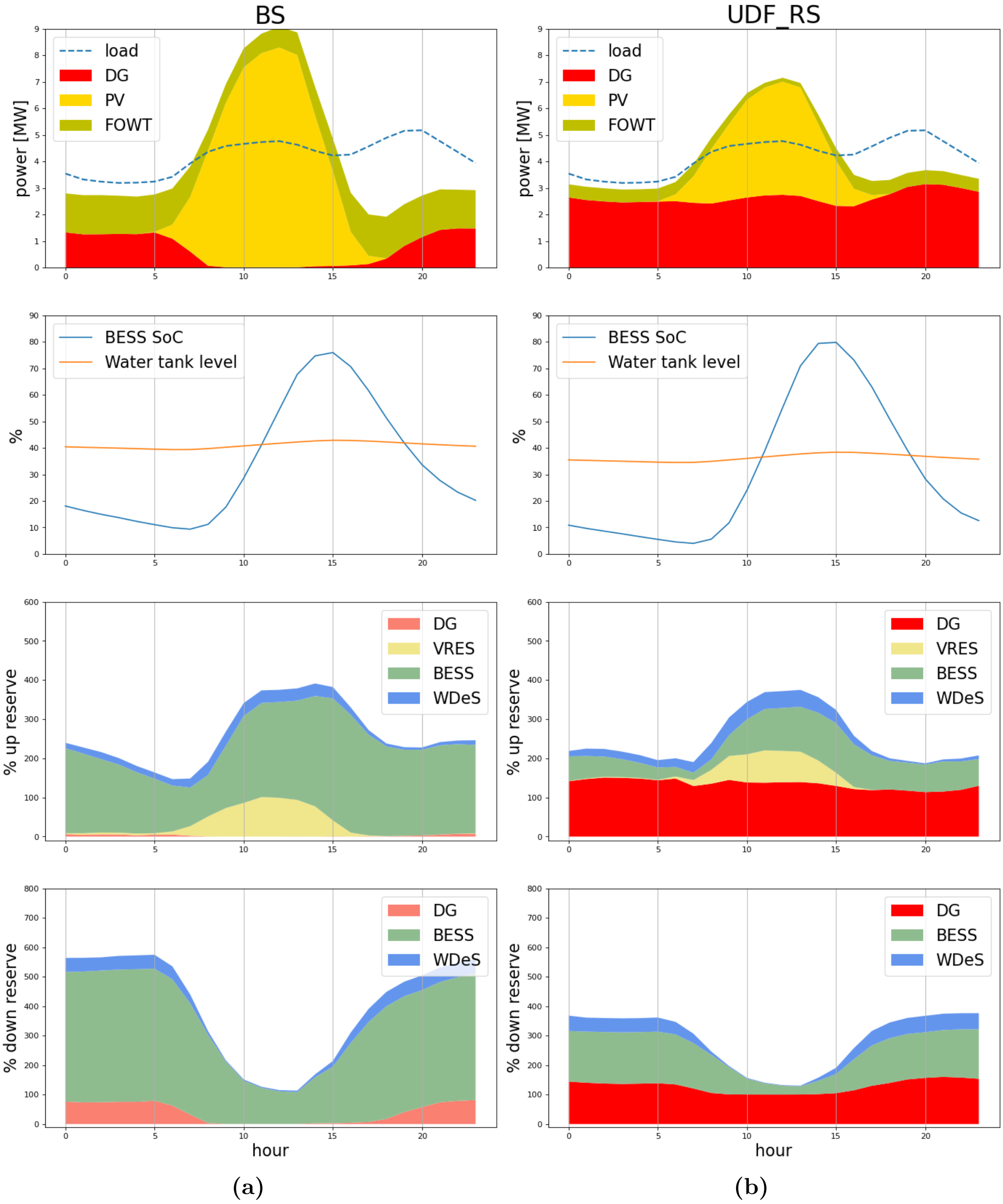

Figure 5.6: Yearly average of each hour of the day for: power and load curves (first row), BESS SoC and water tank level (second row), up and down reserve in relation to the R_{rq} and Q_{rq} requirements (third and fourth rows, respectively), where light colors correspond to the unconstrained reserve in the scenario.

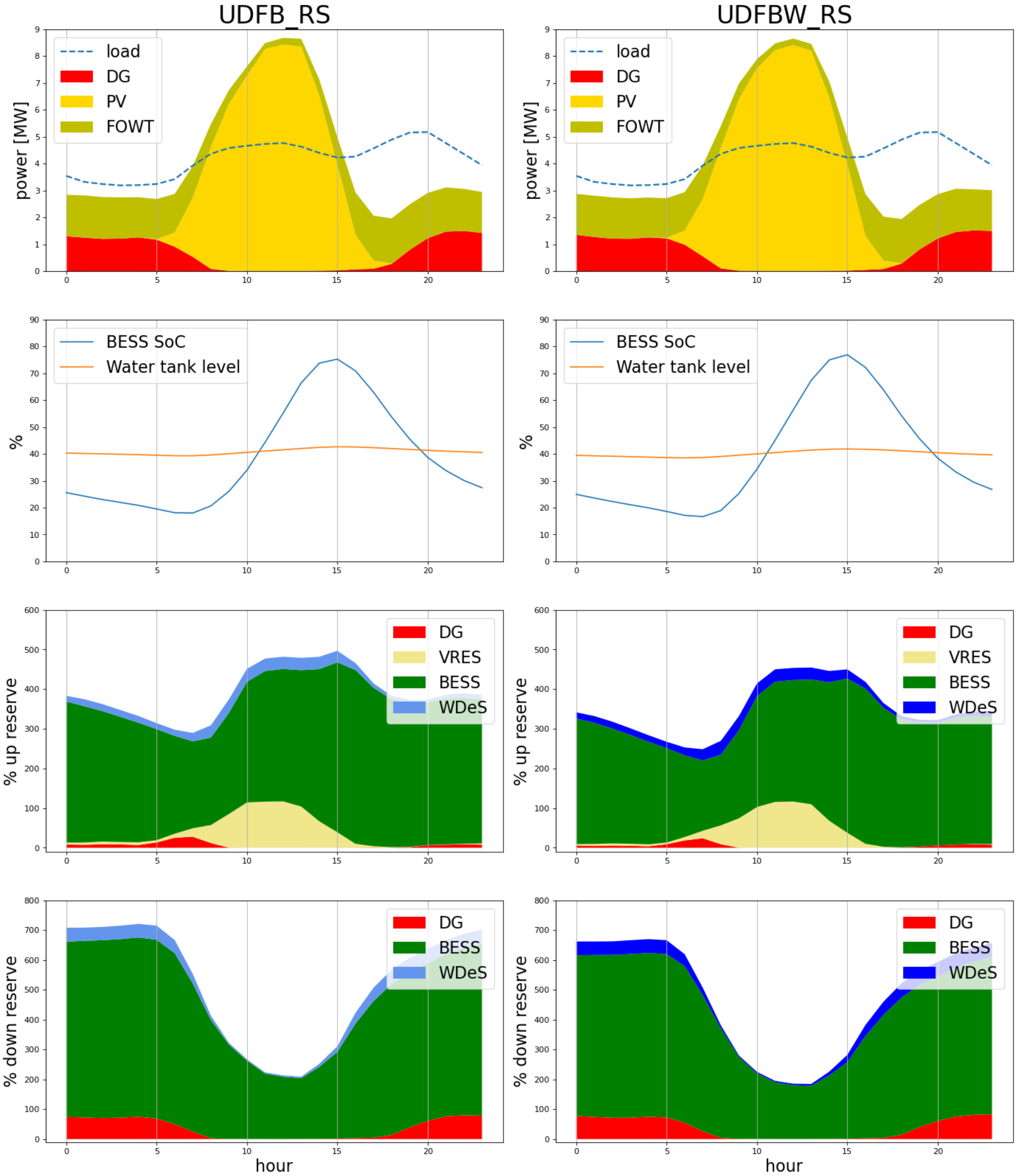

(c) **(d)**

Figure 5.6: Yearly average of each hour of the day for: power and load curves (first row), BESS SoC and water tank level (second row), up and down reserve in relation to the R_{rq} and Q_{rq} requirements (third and fourth rows, respectively), where light colors correspond to the unconstrained reserve in the scenario.

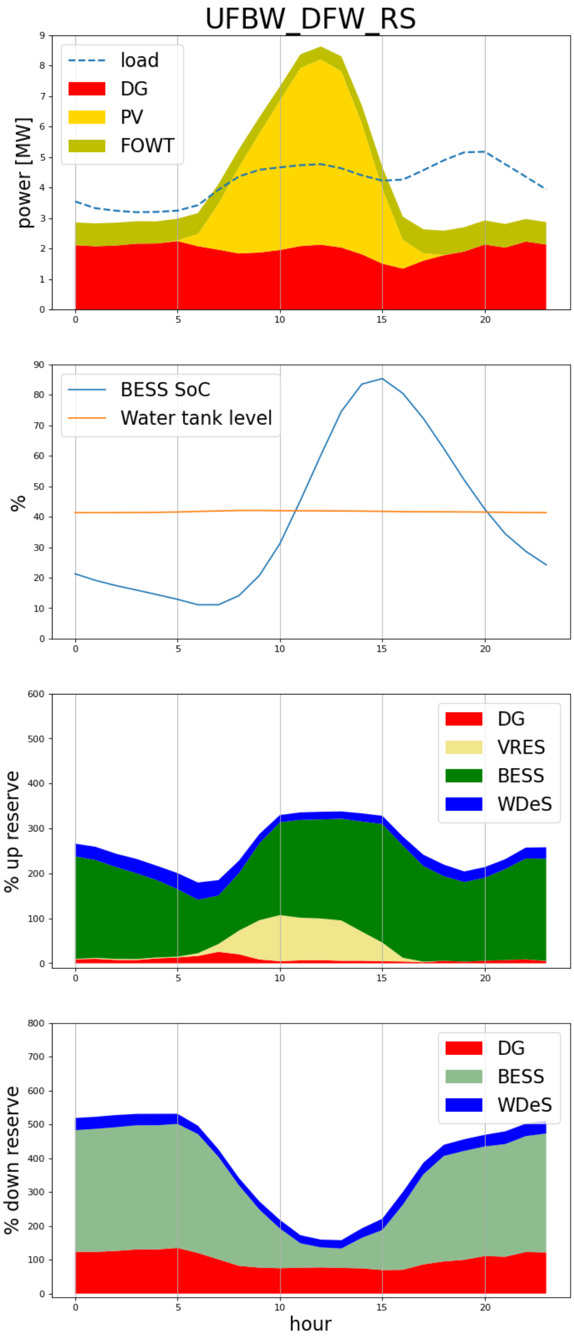

(e)

Figure 5.6: Yearly average of each hour of the day for: power and load curves (first row), BESS SoC and water tank level second row), up and down reserve in relation to the R_{rq} and Q_{rq} requirements (third and fourth rows, respectively), where light colors correspond to the unconstrained reserve in the scenario.

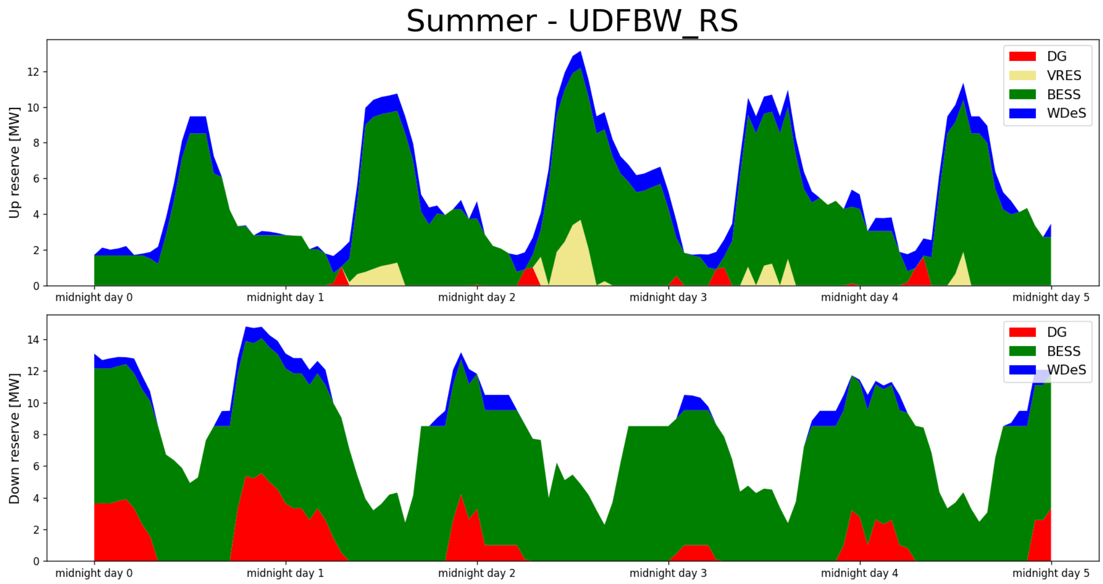

(a)

Figure 5.7: Five-day curves representative of the available reserve in the summer period

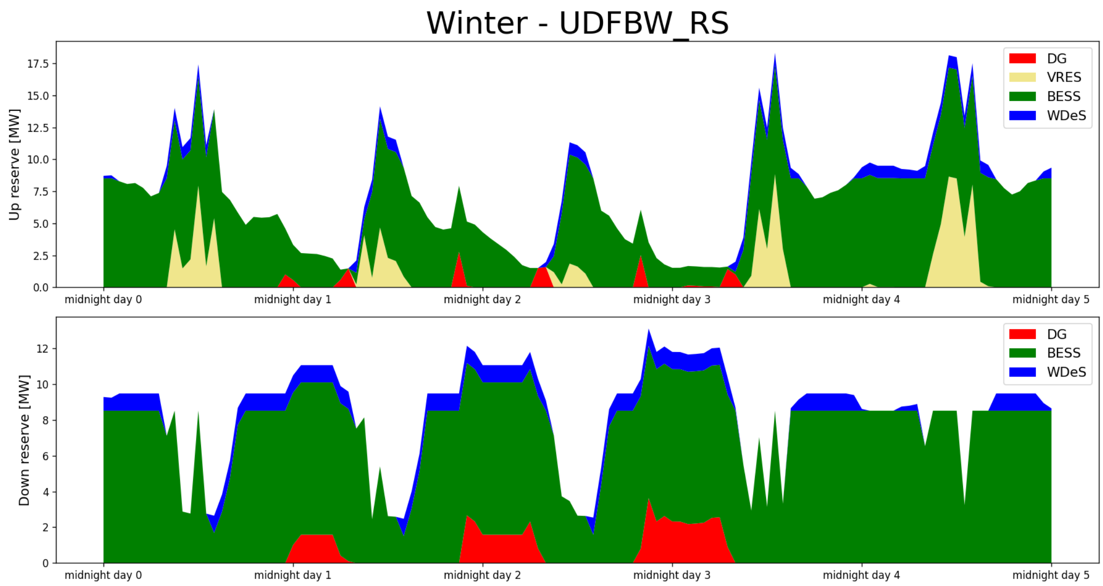

(b)

Figure 5.7: Five-day curves representative of the available reserve in the winter period

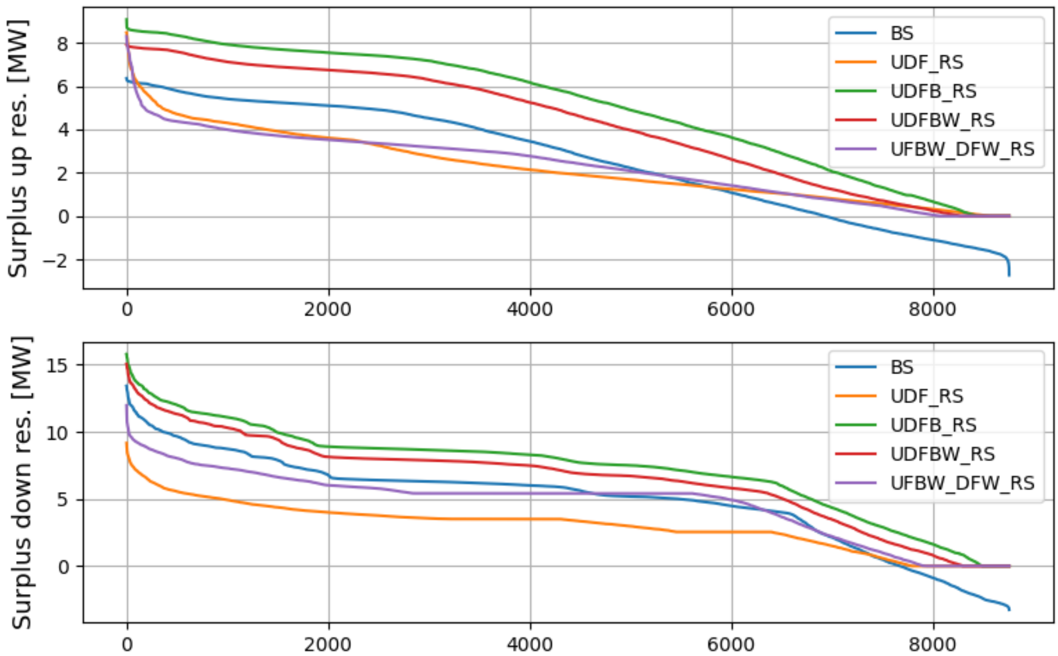

Figure 5.8: Cumulative surplus reserve from DG, BESS and WDeS through the year

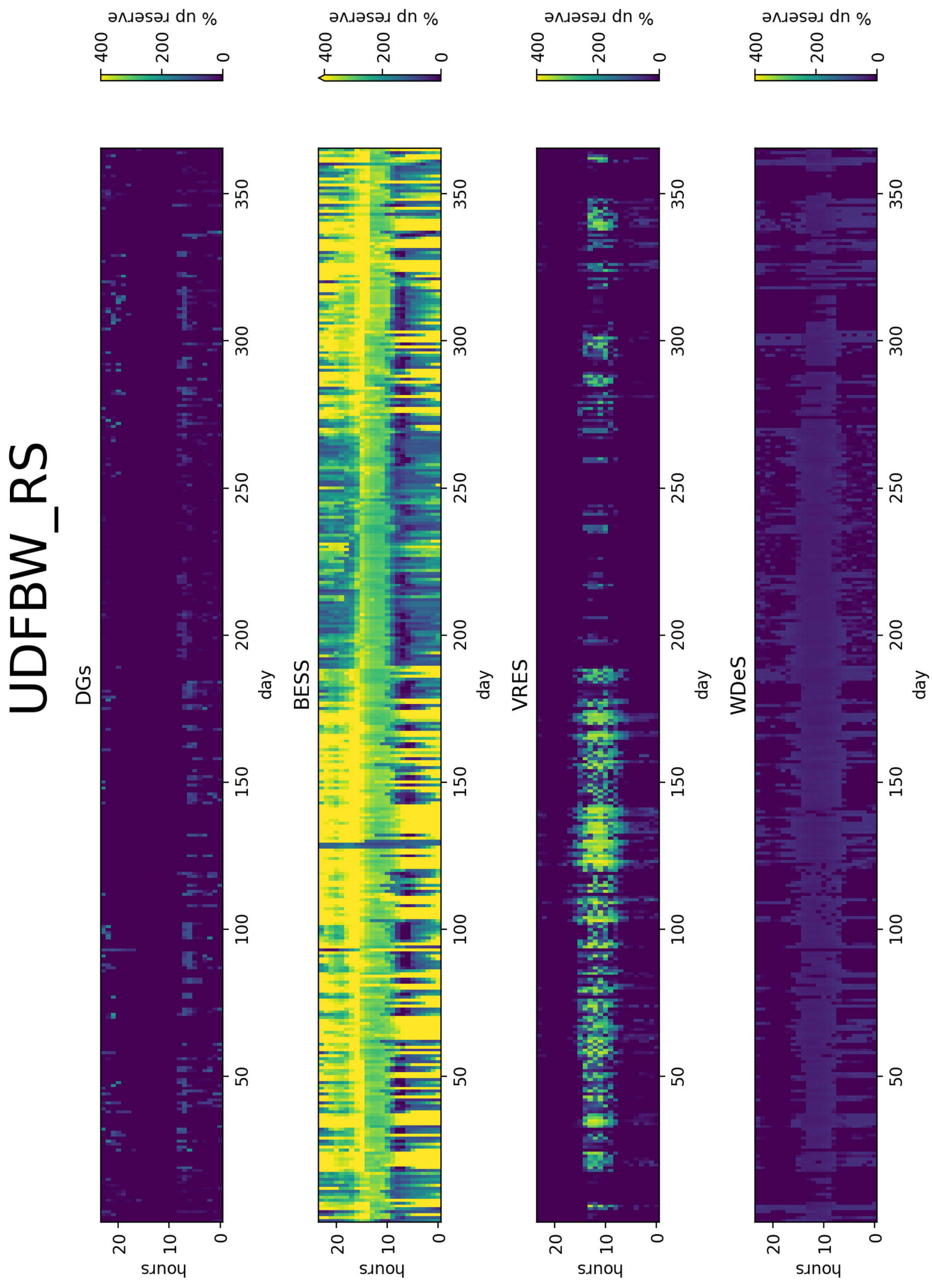

(a)

Figure 5.9: Color map of % up reserve (in relation to R_{rq}) provided by DGs, BESS, WDeS and potential reserve available from VRES.

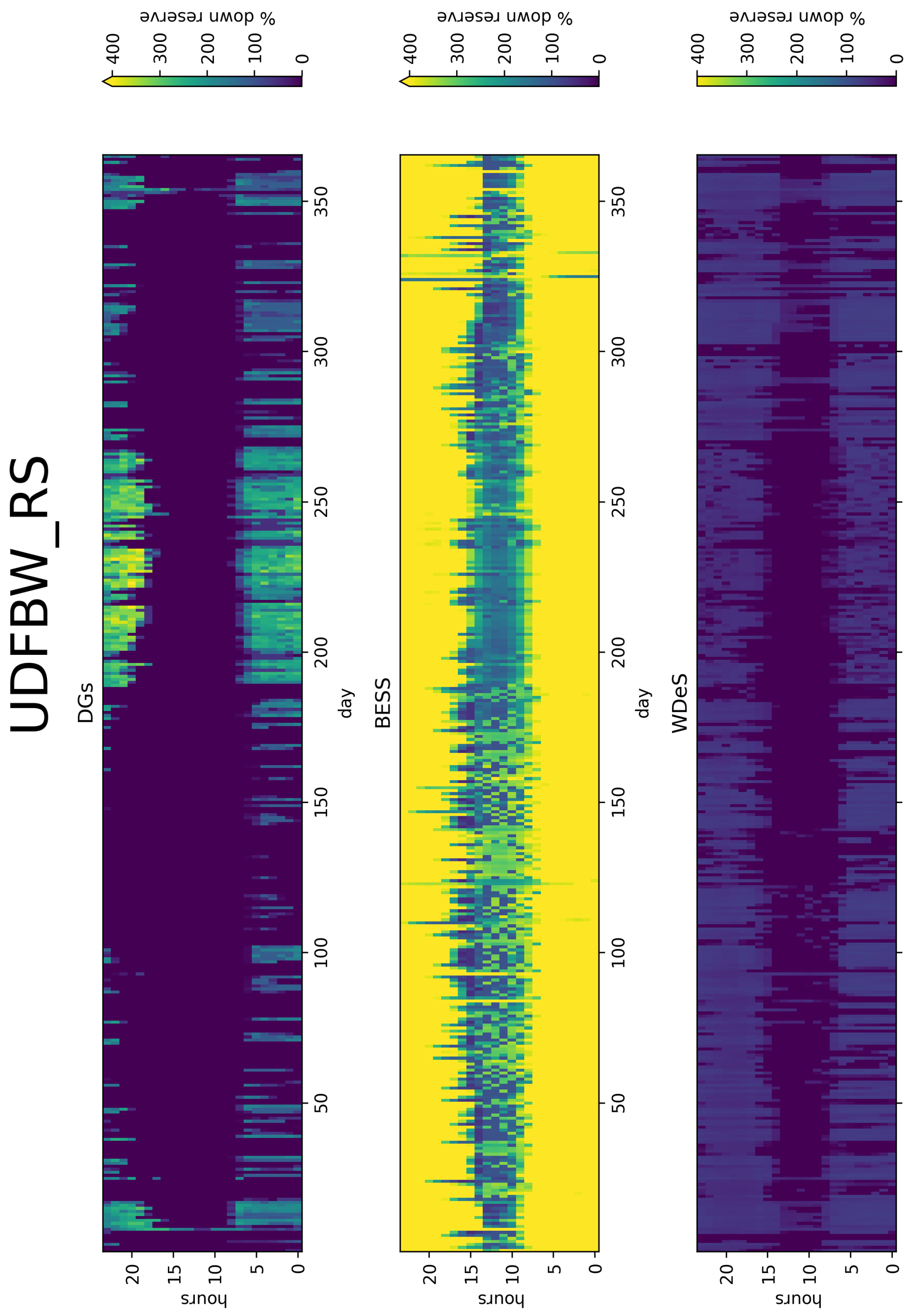

(b)

Figure 5.9: Color map of % down reserve (in relation to Q_{rq}) provided by DGs, BESS, WDeS.

Chapter 6

Conclusions and Future Directions

6.1 Summary and key findings

This work proposes a formulation to incorporate uncertainty and reserve provision into the optimization problem of an off-grid power system. The model includes PV, FOWT, and DG generators, and it can explore power supply strategies while considering network stability. It can simulate water production using WDeS assets, considers storage from Li-Es and water tanks, and simulates electric and water load for a full year.

Islands are ideal for energy planning research due to their isolated nature, limited land resources, abundance of renewable energy sources, and urgent need for sustainable and reliable energy solutions. Consequently, Pantelleria Island was selected as the case study.

Given the limitations discussed in Chapter 4.3, this research aims to evaluate the impacts of Li-Es and water storage when incrementally introducing each asset into the reserve provision. It also compares results considering only up reserve versus both up and down reserves. The effects were analyzed in terms of costs, fuel consumption, reserve availability, and the operational conditions of FFGs and batteries.

Annualized Costs and Fuel consumption Compared to the best scenario, the results show an increase in annualized costs and fuel consumption when only FFGs provide reserve.
Annualized costs and their differences between scenarios decrease when BESS

and WDeS are taken into account, but WDeS do not prove to be a cost-effective substitute for BESS in down reserve provision, although they can help alleviate the workload on FFGs. The contribution of BESS and WDeS, if managed properly, can help save nearly -43% of annual costs and more than -75% of fuel consumption.

Reserve availability Up and down reserves were shown to be inversely proportional, following a 24-hour cycle that changes in magnitude throughout the year. In scenarios where reserve from BESS is included in the Pantelleria network, early morning seems to be the most critical time for up reserve availability, especially during summer, while midday is critical for down reserve with slightly less seasonal variability.
In the context of off-grid power systems, the most capable and economically favorable technology for providing reserve appears to be BESS.

Work Condition of Assets Simulations show that DGs are forced to operate across a broader range of regimes when they are the only technology providing reserve. When BESS and WDeS contribute, the system tries to operate DGs at higher power outputs, thereby improving their efficiency.
The scenario with reserve provided only by DGs shows a greater tendency to charge BESS at the upper limit of their safe charging capacity, where the efficiency of BESS is inversely proportional to the charging or discharging power.

Up vs Up & Down Reserve Simulations Comparison of the results shows that neglecting down reserve can lead to an underestimation of costs and asset sizes, particularly for BESS capacity. Annual costs can be underestimated by nearly -50% if the down reserve is not constrained. The underestimation of assets, on the other hand, results in the need for a +50% more powerful converter in scenarios with both up and down reserve respect to only up reserve when its constrained from FFG and BESS.
Another notable difference is the reversal in the trend for PV and FOWT curtailment. This change appears to be correlated with the reliance on DGs and battery energy capacity. In scenarios with smaller BESS, the system tends to minimize FOWT curtailment, likely due to its consistent output throughout the day. Conversely, with larger battery sizes, PV curtailment tends to decrease.

6.2 Recommendations for future research directions

This study demonstrates the capability of batteries and desalination plants in stabilizing network imbalances and reducing overall costs for off-grid power systems.

By analyzing data collected from Pantelleria Island, an Italian island in the Mediterranean Sea, valuable insights for microgrid optimization have been garnered. Microgrid optimization, which involves improving the efficiency and reliability of a small-scale electric grid, in our case study also aimed to consider balancing supply and demand, integrating renewable energy sources, and minimizing costs. However, it is important to acknowledge the limitations inherent in the study, primarily stemming from the simplified modeling of reserve requirements and the characteristics of generators, storage systems, and the desalinators. Reserve requirements are backup power resources that can be activated to maintain grid stability during unexpected disruptions or demand surges. Accurate modeling of these requirements is crucial for reliable power system operation. The Water Desalination System (WDeS) is a process that removes salts and other impurities from seawater to produce fresh water. Desalination plants are energy-intensive, and their integration into power systems can help stabilize grid imbalances.

Future studies could enhance the modeling of desalination technologies by incorporating more specific data on minimum output power and efficiency curves at different power outputs. This would provide a more accurate representation of how these plants operate under varying conditions. The modeling of water systems should include stagnation times (the time water remains in a storage system without movement) to ensure compliance with regulatory standards. Additionally, the operational schedules of desalination plants should be factored in to optimize water production and storage.
Evaluating the integration of hydrogen production into off-grid systems presents an interesting avenue for research. This includes examining the water consumption required for electrolysis (the process of splitting water into hydrogen and oxygen using electricity) and its impact on overall system efficiency and sustainability. Considering the sizing of desalination plants or hydrogen production facilities in a greenfield scenario. This could involve assessing the optimal scale and configuration of these facilities to meet future demand and sustainability goals. By addressing these areas, future research can provide a more comprehensive and detailed understanding of how to optimize off-grid power systems, particularly in isolated and resource-constrained environments like Pantelleria Island.

Bibliography

[1] Alberto Boretti and Stefania Castelletto. «Trends in performance factors of wind energy facilities». In: *SN Applied Sciences* 2.10 (2020), p. 1718 (cit. on pp. 1, 4).

[2] Živa Bricman Rejc and Marko Čepin. «Estimating the additional operating reserve in power systems with installed renewable energy sources». In: *International journal of electrical power & energy systems* 62 (2014), pp. 654–664 (cit. on p. 1).

[3] Audun Botterud. «Forecasting renewable energy for grid operations». In: *Renewable Energy Integration*. Elsevier, 2017, pp. 133–143 (cit. on p. 2).

[4] Yang Yang, Minglei Bao, Yi Ding, Heping Jia, Zhenzhi Lin, and Yusheng Xue. «Impact of down spinning reserve on operation reliability of power systems». In: *Journal of Modern Power Systems and Clean Energy* 8.4 (2020), pp. 709–718 (cit. on p. 2).

[5] Arne van Stiphout, Kristof De Vos, and Geert Deconinck. «The impact of operating reserves on investment planning of renewable power systems». In: *IEEE Transactions on Power Systems* 32.1 (2016), pp. 378–388 (cit. on p. 2).

[6] Arne Van Stiphout, Kris Poncelet, Kristof De Vos, and Geert Deconinck. «The impact of operating reserves in generation expansion planning with high shares of renewable energy sources». In: *IAEE European Energy Conference, Sustainable Energy Policy and Strategies for Europe, Date: 2014/10/28-2014/10/31, Location: Rome, Italy*. 2014, pp. 1–15 (cit. on p. 2).

[7] Jethro Dowell, Graeme Hawker, Keith Bell, and Simon Gill. «A Review of probabilistic methods for defining reserve requirements». In: *2016 IEEE Power and Energy Society General Meeting (PESGM)*. IEEE. 2016, pp. 1–5 (cit. on p. 2).

[8] Lori Bird, Michael Milligan, and Debra Lew. *Integrating variable renewable energy: Challenges and solutions*. Tech. rep. National Renewable Energy Lab.(NREL), Golden, CO (United States), 2013 (cit. on pp. 3–5).

[9] T. Brown, J. Hörsch, and D. Schlachtberger. «PyPSA: Python for Power System Analysis». In: *Journal of Open Research Software* 6.4 (1 2018). DOI: `10.5334/jors.188`. eprint: `1707.09913`. URL: `https://doi.org/10.5334/jors.188` (cit. on pp. 3, 15).

[10] Semich Impram, Secil Varbak Nese, and Bülent Oral. «Challenges of renewable energy penetration on power system flexibility: A survey». In: *Energy Strategy Reviews* 31 (2020), p. 100539 (cit. on pp. 5, 27).

[11] Md Mustafizur Rahman, Abayomi Olufemi Oni, Eskinder Gemechu, and Amit Kumar. «Assessment of energy storage technologies: A review». In: *Energy Conversion and Management* 223 (2020), p. 113295 (cit. on p. 6).

[12] Behnam Zakeri, Giorgio Castagneto Gissey, Paul E Dodds, and Dina Subkhankulova. «Centralized vs. distributed energy storage–Benefits for residential users». In: *Energy* 236 (2021), p. 121443 (cit. on p. 6).

[13] Rick Wallace Kenyon, Matthew Bossart, Marija Marković, Kate Doubleday, Reiko Matsuda-Dunn, Stefania Mitova, Simon A Julien, Elaine T Hale, and Bri-Mathias Hodge. «Stability and control of power systems with high penetrations of inverter-based resources: An accessible review of current knowledge and open questions». In: *Solar Energy* 210 (2020), pp. 149–168 (cit. on pp. 7, 8).

[14] Stanislav Misak and Lukas Prokop. «Off-grid power systems». In: *2010 9th International conference on environment and electrical engineering*. IEEE. 2010, pp. 14–17 (cit. on p. 7).

[15] Godfrey Gladson Moshi, Cristian Bovo, and Alberto Berizzi. «Optimal operational planning for PV-Wind-Diesel-battery microgrid». In: *2015 IEEE Eindhoven PowerTech*. IEEE. 2015, pp. 1–6 (cit. on p. 8).

[16] Enrico Giglio, Riccardo Novo, Giuliana Mattiazzo, and Davide Fioriti. «Reserve provision in the optimal planning of off-grid power systems: impact of storage and renewable energy». In: *IEEE Access* (2023) (cit. on pp. 8, 9, 11, 13, 21).

[17] IBM. «V12.7: User's Manual (IBM ILOG CPLEX Division, Incline Village, NV)». In: *International Business Machines Corporation* (2017) (cit. on p. 11).

[18] Gurobi Optimization, LLC. *Gurobi Optimizer Reference Manual*. 2023. URL: `https://www.gurobi.com` (cit. on p. 11).

[19] Wesley J Cole and Allister Frazier. *Cost projections for utility-scale battery storage*. Tech. rep. National Renewable Energy Lab.(NREL), Golden, CO (United States), 2019 (cit. on pp. 12, 20, 23).

[20] Bjarne Steffen. «Estimating the cost of capital for renewable energy projects». In: *Energy Economics* 88 (2020), p. 104783. ISSN: 0140-9883. DOI: `https://doi.org/10.1016/j.eneco.2020.104783`. URL: `https://www.sciencedirect.com/science/article/pii/S0140988320301237` (cit. on p. 17).

[21] ISOLA DI PANTELLERIA. «AGENDA PER LA TRANSIZIONE ENERGETICA». In: (2020) (cit. on pp. 18, 21).

[22] Christopher S Stokes, Holger R Maier, and Angus R Simpson. «Effect of storage tank size on the minimization of water distribution system cost and greenhouse gas emissions while considering time-dependent emissions factors». In: *Journal of Water Resources Planning and Management* 142.2 (2016), p. 04015052 (cit. on p. 19).

[23] Yixin Liu, Li Guo, Ruosong Hou, Chengshan Wang, and Xiaoxue Wang. «A hybrid stochastic/robust-based multi-period investment planning model for island microgrid». In: *International Journal of Electrical Power Energy Systems* 130 (2021), p. 106998. ISSN: 0142-0615. DOI: `https://doi.org/10.1016/j.ijepes.2021.106998`. URL: `https://www.sciencedirect.com/science/article/pii/S0142061521002386` (cit. on p. 19).

[24] Claudio Moscoloni, Fernando Zarra, Riccardo Novo, Enrico Giglio, Alberto Vargiu, Guglielmina Mutani, Giovanni Bracco, and Giuliana Mattiazzo. «Wind turbines and rooftop photovoltaic technical potential assessment: Application to sicilian minor islands». In: *Energies* 15.15 (2022), p. 5548 (cit. on p. 20).

[25] Iain Staffell and Stefan Pfenninger. «Using bias-corrected reanalysis to simulate current and future wind power output». In: *Energy* 114 (2016), pp. 1224–1239 (cit. on p. 20).

[26] Stefan Pfenninger and Iain Staffell. «Long-term patterns of European PV output using 30 years of validated hourly reanalysis and satellite data». In: *Energy* 114 (2016), pp. 1251–1265 (cit. on p. 20).

[27] H Hersbach, B Bell, P Berrisford, S Hirahara, A Horányi, and J Muñoz-Sabater. «The ERA5 global reanalysis, quarterly journal of the royal meteorological society». In: (2020) (cit. on p. 20).

[28] Matt Shields, Patrick Duffy, Walt Musial, Michael Laurienti, Donna Heimiller, Rob Spencer, and Mike Optis. *The Costs and Feasibility of Floating Offshore Wind Energy in the O'ahu Region*. Tech. rep. National Renewable Energy Lab.(NREL), Golden, CO (United States), 2021 (cit. on p. 20).

[29] Laura Vimmerstedt et al. *Annual technology baseline: The 2022 electricity update*. Tech. rep. National Renewable Energy Lab.(NREL), Golden, CO (United States), 2022 (cit. on p. 20).

[30] International Renewable Energy Agency IRENA. *Renewable power generation costs in 2020*. eBook Partnership, 2022 (cit. on p. 20).

[31] Albert H Zimmerman. «Self-discharge losses in lithium-ion cells». In: *IEEE Aerospace and Electronic Systems Magazine* 19.2 (2004), pp. 19–24 (cit. on p. 20).

[32] Faraedoon Ahmed, Dlzar Al Kez, Seán McLoone, Robert James Best, Ché Cameron, and Aoife Foley. «Dynamic grid stability in low carbon power systems with minimum inertia». In: *Renewable Energy* 210 (2023), pp. 486–506 (cit. on p. 20).

[33] *R01 Relazione tecnica e di indagine idraulica.pdf*. Online. URL: `https://www.comunepantelleria.it/gare/72676541CF/R01%20Relazione%20tecnica%20e%20di%20indagine%20idraulica.pdf` (cit. on p. 21).

[34] Riccardo Novo, Francesco Demetrio Minuto, Giovanni Bracco, Giuliana Mattiazzo, Romano Borchiellini, and Andrea Lanzini. «Supporting decarbonization strategies of local energy systems by de-risking investments in renewables: a case study on pantelleria island». In: *Energies* 15.3 (2022), p. 1103 (cit. on p. 21).

[35] Fabian Hofmann. «Linopy: Linear optimization with n-dimensional labeled variables». In: *Journal of Open Source Software* 8.84 (2023), p. 4823. DOI: `10.21105/joss.04823`. URL: `https://doi.org/10.21105/joss.04823` (cit. on p. 22).

[36] Friedrich B Jasper, Jana Späthe, Manuel Baumann, Jens F Peters, Janna Ruhland, and Marcel Weil. «Life cycle assessment (LCA) of a battery home storage system based on primary data». In: *Journal of Cleaner Production* 366 (2022), p. 132899 (cit. on p. 23).

[37] Nikolay Voutchkov et al. «Desalination engineering: planning and design». In: *(No Title)* (2013) (cit. on p. 23).